

Southern Boundary Restoration & Enhancement Fund 2006/2007

**Project SF-2006-I-21
Determining Canadian MU-Specific Reference Points**

PREPARED BY

Josh Korman,
Ecometric Research
3560 West 22nd Ave
Vancouver, BC V6S 1J3
and
Arlene Tompkins,
Fisheries and Oceans Canada
Pacific Biological Station,
3190 Hammond Bay Rd
Nanaimo, BC V9T 6N7

June 13, 2007

Determining Canadian MU-Specific Reference Points

Part 1:

Estimating Regional Distributions of Freshwater Stock Productivity, Carrying Capacity, and Sustainable Harvest Rates for Coho Salmon Using a Hierarchical Bayesian Modelling Approach

Abstract

We estimated regional distributions of freshwater productivity and carrying capacity for coho salmon to support a forthcoming modeling effort to evaluate the efficacy of alternate fixed harvest rate and abundance-based harvest rate policies. The objectives of this analysis were to: determine the most suitable form of the stock-recruitment model using information theoretic criteria; estimate and compare regional distributions of stock-recruitment parameters from alternate models; estimate regional distributions of sustainable harvest rates under different marine survival regimes; and to evaluate the validity of applying the regional stock-recruitment distributions to populations in the Georgia Basin West management unit and the Thompson River drainage. We used a hierarchical Bayesian modeling approach because it correctly weights the contribution of each population to the regional distribution based on its information content.

We compiled spawner-to-smolt data from 17 coastal populations of coho salmon in Oregon, Washington, and BC (n=259). Beverton-Holt (BH), Ricker (RI), and Logistic Hockey Stick (LHS) models fit the data well and were consistent with the assumed lognormal error structure. In cases where there was little decline in smolt abundance at low stock size, the BH model estimated unrealistically high stock productivities, while the Ricker model estimated lower productivities by overestimating the magnitude of overcompensation. The LHS model avoided both these pitfalls, fit the data best and had the highest out-of-sample predictive power. There was essentially no support for the Ricker model based on both Akaike and Deviance Information criteria, and only moderate support for the BH model based on the latter criteria.

The mean of the most likely regional distributions of stock productivity and carrying capacity based on BH, LHS, and RI models were 86, 58, and 43 smolts/spawner, and 1397, 1154, and 1357 smolts/km, respectively. Although there was strong covariation among stock productivity and carrying capacity estimates within populations, there was no relationship across populations under both hierarchical and non-hierarchical models. Due to data limitations for some populations, it was uncertain whether they had lower carrying capacity and higher productivity or visa-versa. However, this does not imply that more productive populations tend to have lower capacities (or visa-versa).

Prior probabilities for the means of regional distributions of stock productivity and carrying capacity were very uninformative and had no influence on the resulting maximum likelihood estimates of hyper-parameters. However, in the absence of a weakly informative prior on the lower limit of across-population variation in stock productivity and carrying capacity, the hierarchical model would estimate an unrealistically low variance for one of the two parameters by inflating the variance estimate for the other. The means and medians of the marginal distributions for stock productivity and carrying capacity for the Logistic Hockey Stick model were 79 and 65 smolts/spawner and 1642 and 1292 smolts/km, respectively.

Regional distributions of harvest rate (U_{msy}) and spawner densities (S_{msy}) that resulted in maximum sustainable yields were computed based on samples from the marginal predictive distributions of stock productivity and carrying capacity. As expected, U_{msy} declined considerably at lower marine survival rates (m_s). In the worst scenario ($m_s=0.025$), 20% of the populations were unsustainable even in the absence of harvest. Modal U_{msy} values at $m_s=0.025$, 0.05, and 0.10 were 0.3, 0.6, and 0.7, respectively. Escapement to achieve MSY increased at higher marine survival rates. U_{msy} predictive distributions varied considerably among stock-recruitment models. At low marine survival ($m_s=0.025$), the Beverton-Holt model predicted higher U_{msy} 's relative to the other models. U_{msy} distributions for BH and LHS models were similar at marine survival rates of 0.05 and 0.1. The Ricker model predicted the most conservative U_{msy} distribution under all marine survival regimes.

The product of mean smolt capacity per km of stream (from the marginal distribution) and total accessible stream length underpredicted adult carrying capacity by about 2-fold for GBW and overestimated capacity by a similar magnitude for the Thompson River drainage. In the case of the Thompson, it is possible that the total amount of stream length used for coho rearing was overestimated because larger mainstem reaches comprised about 50% of the total. There was good agreement between predicted and backcalculated adult carrying capacity when 6th and 7th order reaches were removed. In the case of GBW, accessible stream length could have been underestimated, as many productive side-channel habitats would not be shown on a 1-50,000 map-scale. Alternately, the habitat model may be correct and backcalculated adult capacity could be

overestimated because escapement data included hatchery contributions. In the absence of reliable estimates of naturally produced escapement, the comparison of predicted and observed carrying capacities for GBW remains very inconclusive.

Aggregate escapements for GBW and the Thompson River were simulated based on historical exploitation and marine survival rates and random draws from the marginal distributions of stock-recruitment parameters. Predicted escapements underestimated observed values and tended to overpredict the extent of population decline. The analysis suggests that the index streams used to generate the marginal distributions of stock-recruitment parameters do not overrepresent productive populations in GBW or the Thompson River. This conclusion should be considered preliminary as marine survival and exploitation rates for Thompson populations are uncertain, and the GBW escapement data contains temporally varying and large but unknown hatchery contributions. However, given uncertainties in the data and the conservative nature of model predictions to harvest, it seems reasonable to use the regional distributions of carrying capacity and stock productivity developed from this hierarchical meta-analysis to represent the population dynamics for GBW and Thompson River in a forthcoming harvest rate analysis.

1.0 Introduction

A group of populations with different productivities will exhibit highly divergent responses to a common harvest regime. At an intermediate harvest rate, weak or unproductive populations will be depleted and possibly extirpated, while highly productive ones will be underexploited. Under fixed escapement or abundance-based harvest rate policies, the carrying capacity of individual populations must also be considered. Conservation concerns for coho salmon in Southern British Columbia require that harvest regimes be evaluated based on the response of multiple populations in a management unit, rather than on the aggregate response. Evaluation of harvest regimes in this setting therefore requires estimation of distributions that reflect the variation in carrying capacity and stock productivity among populations. The objective of this analysis is to define regional distributions of freshwater productivity and carrying capacity for coho salmon in Southern BC to evaluate the efficacy of a range of fixed harvest rate and abundance-based harvest rate policies.

In this analysis, carrying capacity is defined, as the number of smolts produced per length of accessible stream when spawning stock size is not limiting. Capacity will be determined by the amount of habitat and the nature of compensatory mortality. Stock productivity is defined as the slope at the origin of the spawner-to-smolt relationship and is determined by density-independent mortality rates. The product of freshwater stock productivity and marine survival rate will determine the maximum sustainable harvest rate and the rate at which populations recover from overharvesting or extended periods of low marine survival. The use of an abundance-based harvest rate rule as recommended by the Pacific Salmon Commission (PSC 2004) requires an estimate of the carrying capacity for each management unit. This can be calculated by multiplying a length-standardized carrying capacity estimate by the total productive stream length in the management unit. The product of total smolt production for a management unit and marine survival define adult recruitment carrying capacity that in turn can be used as a reference point to define specific harvest rate thresholds according to abundance-based harvest rules.

Dramatic declines in coho escapements have motivated much analysis of existing stock-recruitment data, and some of these analyses have focused on estimating regional distributions of stock productivity and capacity. In this analysis we improve on past

efforts using extended datasets and a hierarchical Bayesian approach. Bradford et al. (2000) developed regional distributions of freshwater productivity and capacity for coho salmon by computing the mean and variance of stock-recruitment parameters estimated individually for each of 14 coho populations. Barrowman et al. (2003) and Chen and Holtby (2002) show that such an approach can lead to overestimates of the mean and variance of regional distributions, leading in turn to overestimates of the sustainable harvest rate. The form of the stock-recruitment model has been shown to have a large influence on stock productivity and carrying capacity estimates (Barrowman and Myers, 2000). The use of hockey stick and Ricker stock-recruitment models in the analyses of Bradford et al. (2000) and Chen and Holtby (2002) to estimate regional distributions of stock productivity were not rigorously supported. The hockey stick model, with its abrupt transition, is poorly suited for estimating uncertainty in stock-recruitment parameters, an essential element for determining regional distributions (Barrowman et al. 2003). The Ricker, and especially the Beverton-Holt model, potentially overestimate stock productivity in cases where there is little information about recruitment at low stock size (Barrowman and Myers 2000). Chen and Holtby (2002) concurred with this assessment of the Beverton-Holt model for coho salmon, but concluded that the Ricker model could provide reasonable estimates of stock productivity for management purposes. They used the Ricker model because it produced lower estimates of stock productivity leading to more conservative harvest rates. Model selection should be based on objective statistical criteria (Burnham and Anderson 2002) or close-looped policy performance (Walters and Martell 2004).

The objectives of this analysis are to: 1) determine the most suitable form of a stock-recruitment model for the freshwater phase of coho salmon based on a rigorous assessment of the fit and biases of alternate models; 2) to estimate and compare regional distributions of stock productivity and smolt carrying capacity based on alternate stock-recruitment models in a Bayesian hierarchical modeling framework; 3) to estimate regional distributions of sustainable harvest rates under different marine survival regimes; and to 4) evaluate the validity of applying the regional stock-recruitment distributions to populations in the Georgia Basin West management unit and the Thompson River drainage. The main advantage of a hierarchical model is that it correctly weights the

contribution of each population to the regional distribution based on its information content. For example, stock productivity estimates will be highly uncertain for populations where there is little information about smolt production at low escapement. It makes little sense that parameter estimates in these cases should contribute equally to the regional distribution relative to other populations where stock productivity is better determined from the data. This is why hierarchical models tend to produce regional parameter distributions that often have less variance (sometimes referred to as ‘shrinkage’), and lower means than those developed by estimating parameters individually for each population (e.g. Chen and Holtby 2002), and why estimates of independently-derived regional distributions such as those in Bradford et al. (2000) have been criticized. By using a Bayesian hierarchical model to objectively assess alternate stock-recruitment models, this analysis addresses limitations of the two previously published estimates of regional distributions of stock-recruitment parameters for coho salmon (Chen and Holtby 2002, Bradford et al. 2000).

2.0 Methods

We use a hierarchical Bayesian model to jointly estimate population-specific stock-recruitment parameters as well as hyper-parameters that define their regional distributions. The regional distributions of productivity and carrying capacity are of direct interest in this analysis. Population-specific estimates are considered nuisance parameters but need to be estimated to determine regional distributions. The data (section 2.1), model structure (2.2), and methods for model estimation (2.3), model comparison (2.4), and evaluation of applicability of regional distributions for the Georgia Basin West (GBW) management unit (MU) and the aggregate Thompson River stock (2.5) are described below.

2.1 Data

We compiled spawner-to-smolt data from 17 coastal populations in Oregon, Washington, and BC (Table 1). The majority of these data were first analyzed by Bradford et al. (2000). In this analysis, we have updated data sets from Big Beef, Black, Carnation, and Snow Creeks and included data from two new systems (Queets and Skagit Rivers). While the abundance of spawners and smolts are relatively well determined in

these streams, the populations may not provide a representative sample for all BC management units because: 1) the sample may over-represent stocks with higher productivity and/or carrying capacity (Bradford et al. 2000); and 2) the majority of streams in the dataset are coastal systems in Washington and Oregon and may therefore not be representative of coastal coho populations and especially interior populations, in British Columbia.

The alternate dataset to estimate regional distributions of stock productivity and carrying capacity is the DFO salmon escapement data (SEDS), which includes information for tens to hundreds of streams within each management unit. Due to its extensive coverage, the SEDS data in theory would allow better definition of regional distributions (e.g., Chen and Holtby 2002). However, distributions developed from the SEDS data will be highly uncertain because of methodological problems and inconsistencies in escapement estimates within and among streams over time. In addition, to back-calculate smolt recruitment from escapement requires application of uncertain exploitation and marine survival rates (e.g., Folkes et al. 2005). Such estimates are available for only a few stocks and typically for shorter time periods than the period over which escapement data is generally available.

In this analysis we estimate regional distributions of stock productivity and carrying capacity using spawner-to-smolt data only. These data have considerably less observation error than SEDS data and are therefore more useful for determining the best form of the stock-recruitment relationship and the regional distribution of stock-recruitment parameters. However, we use SEDS data from populations in the GBW management unit and the Thompson River to evaluate whether regional distributions of stock-recruitment parameters developed from the spawner-to-smolt data can reproduce trends in the aggregate escapement in these areas.

2.2 Model Structure

We evaluated fits of the Beverton-Holt (BH), Logistic Hockey Stick (LHS), and Ricker stock-recruitment models to the spawner-to-smolt data. The form of the Beverton-Holt applied here (following Sharma and Hilborn 2001) is:

$$(1) \quad R_{i,t} = \frac{S_{i,t-2}}{\frac{1}{\alpha_i} + \frac{S_{i,t-2}}{\beta_i}}$$

where, $R_{i,t}$ is the number of smolts from population ‘i’ in year ‘t’, $S_{i,t-2}$ are the number of spawners for the same population in year t-2, α_i is the initial slope of the line and is equivalent to the number of smolts produced per spawner at low density (stock productivity), and β_i is the maximum number of smolts that can be produced from the population per km of stream when stock size is not limiting (carrying capacity). The form of the Ricker model (RI) used here is:

$$(2) \quad R_{i,t} = \alpha_i S_{i,t-2} e^{-\delta_i S_{i,t-2}}$$

where, δ_i is the reduction in survival due to increasing density. In this analysis, estimation of β_i (maximum recruitment) is of interest and is calculated from $\frac{\alpha_i}{\delta_i} e^{-1}$ (Hilborn and Walters 1992). This parameterization is convenient because the interpretation of the estimated parameters α_i and β_i is consistent across stock-recruitment models.

The form of the Logistic Hockey Stick model (LHS, Barrowman and Myers 2000) is:

$$(3) \quad R_{i,t} = \alpha_i C \delta_i (1 + e^{\frac{-1}{C}}) \left[\frac{S_{i,t-2}}{C \delta_i} - \log\left(\frac{1 + e^{\frac{(S_{i,t-2} - \delta_i)/(C \delta_i)}{1 + e^{\frac{-1}{C}}}}}{1 + e^{\frac{-1}{C}}}\right) \right]$$

where,

$$(4) \quad \delta_i = \frac{\beta_i}{\alpha_i} \left[C(1 + e^{\frac{-1}{C}}) \left(\frac{1}{C} + \log(1 + e^{\frac{-1}{C}}) \right) \right]^{-1}$$

As for the previous stock-recruitment models α_i and β_i are estimated. C is a tuning parameter that determines the smoothness at the transition between the initial slope at low stock size and the asymptote at higher stock size. The logistic hockey stick model approaches the hockey stick model as $C \rightarrow 0$. In this analysis the tuning parameter was held constant at $C=1$.

2.3 Estimation

Stock-recruitment parameters were estimated by assuming that residuals of log-transformed data were normally distributed. The likelihood of observing $R_{i,t}$ smolts given a set of parameter estimates is:

$$(5) \quad L(R_{i,t} | \alpha_i, \beta_i, \sigma_i) = \frac{1}{\sqrt{2\pi\sigma_i^2}} e^{-\left[\frac{[\log(R_{i,t}) - \log(\hat{R}_{i,t})]^2}{2\sigma_i^2} \right]}$$

where, $\hat{R}_{i,t}$ is the predicted number of smolts from eqn.'s 1, 2, or 3, and σ_i is the estimated standard deviation of the residuals around the stock-recruitment relationship. σ_i represents variation in freshwater survival rate (i.e., process error) as we assume there is no observation error in the data.

Log-transformed population-specific parameter estimates of stock productivity and carrying capacity are assumed to come from normal hyper-distributions:

$$(6) \quad \begin{aligned} P(\log(\alpha_i)) &\sim N(\log(\mu_\alpha), CV_\alpha) \\ P(\log(\beta_i)) &\sim N(\log(\mu_\beta), CV_\beta) \end{aligned}$$

Hyper-parameter means μ_α and μ_β , and relative variances CV_α and CV_β define the regional (i.e., hyper) distributions for stock productivity and carrying capacity, respectively. Note that unlike Chen and Holby (2002), the model structure does not assume that there is a correlation between stock productivity and carrying capacity across populations.

In empirical Bayes' methods, hyper-parameters would be estimated from related populations but then treated as fixed and known in subsequent estimation of population-specific parameters (e.g., Chen and Holtby 2002). In this analysis, which uses a Bayesian approach, hyper-parameters and nuisance stock-specific parameters are jointly estimated. Priors for the hyper-distribution parameters, or hyper-priors, denoted as $P(\mu_\alpha)$ $P(CV_\alpha)$, $P(\mu_\beta)$, and $P(CV_\beta)$, must therefore be specified. Hyper-priors for the means of the hyper-distributions are assumed to follow a normal distribution with means $\mu(\mu_x)$ and coefficient of variation $CV(\mu_x)$:

$$(7) \quad \begin{aligned} P(\mu_\alpha) &\sim N(\mu(\mu_\alpha), CV(\mu_\alpha) * \mu(\mu_\alpha)) \\ P(\mu_\beta) &\sim N(\mu(\mu_\beta), CV(\mu_\beta) * \mu(\mu_\beta)) \end{aligned}$$

Variances of the hyper-distributions are assumed to follow an inverse gamma distribution (Gelman et al. 2003, Appendix A) with means $\mu(CV_x)$ and precision $\tau(CV_x)$.

$$(8) \quad P(CV_\alpha) \sim \text{Inv-Gamma}(\mu(CV_\alpha), \tau(CV_\alpha))$$

$$P(CV_\beta) \sim \text{Inv-Gamma}(\mu(CV_\beta), \tau(CV_\beta))$$

Uniform prior distributions were specified for population-specific β_i , and σ_i . A very diffuse normal prior on population-specific stock productivity $P(\alpha_i)$ was required to provide numerical stability for the Beverton-Holt model,

$$(9) \quad P(\log(\alpha_i)) \sim N(\log(\mu_{\alpha_i}), CV_{\alpha_i})$$

Prior distributions for almost all parameters were very uninformative (Table 2).

Parameters for the inverse-gamma distributions were chosen to limit the probability of very low inter-population variability in stock productivity and carrying capacity. This parameterization is reasonable, and was necessary to provide numerical stability during the estimation.

The total probability of parameter values given the data is the product of the prior probabilities for the parameters and hyper-parameters, the probability of the population-specific parameter estimates given the hyper-parameters, and the likelihood of the data given the population-specific parameter estimates:

$$(10) \quad P(\alpha_i, \beta_i, \sigma_i, \mu_\alpha, CV_\alpha, \mu_\beta, CV_\beta | R_{i,t}) = P(\alpha_i)P(\mu_\alpha)P(CV_\alpha)P(\mu_\beta)P(CV_\beta) \prod_i P(\alpha_i | \mu_\alpha, CV_\alpha) \prod_i P(\beta_i | \mu_\beta, CV_\beta) \prod_{i,t} L(R_{i,t} | \alpha_i, \beta_i, \sigma_i)$$

Parameters were estimated by minimizing the sum of the negative logs of eqn. 10 using the AD Model Builder (ADMB) software. A total of 55 parameters ($K=55$) are estimated for the hierarchical model ($K= 3$ parameters per population * 17 populations = 51 population-specific parameters + 4 regional parameters). For comparison, population-specific parameters were estimated using a non-hierarchical model ($K=51$) that assumes complete independence among populations (as in Bradford et al. 2000). In this case the total probability was determined based solely on the data from:

$$(11) \quad P(\alpha_i, \beta_i, \sigma_i | R_{i,t}) = \prod_{i,t} L(R_{i,t} | \alpha_i, \beta_i, \sigma_i)$$

The joint posterior distribution of parameters for the hierarchical model was estimated using Markov Chain Monte Carlo (MCMC) simulation in ADMB. A total of 5,000 samples were taken every 100th trial out of a total of 500,000 simulations. The procedure was repeated for two independent Markov chains that were initiated with

highly divergent initial parameter values (high productivity-low capacity or low productivity-high capacity) and different random number seeds. A series of diagnostics implemented in the CODA package written for the R statistical software program were applied to the MCMC samples to evaluate convergence within and across-chains for regional parameters, and to determine the number of initial draws to be discarded (MCMC burn-in). Diagnostics included: Gelman and Rubin’s potential scale reduction factor; Geweke’s test for equality of means; and Heidelberger and Welch’s and Raftery and Lewis’s run length control diagnostics (see Gelman et al. 2003, Section 11.6). Final posterior distributions were based on a total of 5,000 samples by combining the second half of each Markov chain.

The most likely estimates of the regional distributions of stock productivity and carrying capacity do not include the uncertainty in hyper-parameter estimates and will therefore underestimate the extent of across-population variance. It is therefore necessary to estimate the marginal predictive posterior for α_i and β_i (e.g., McAllister et al. 2004). To do this, 10,000 sets of hyper-parameter values were randomly drawn from the joint posterior distribution with each pair defining a regional distribution of stock productivity and carrying capacity. A single random draw from each of the 10,000 distributions was then taken to define population-specific productivity and carrying capacity. These values were aggregated over all draws to generate marginal posterior distributions for α_i and β_i .

2.4 Model-Fit and Comparisons

Model-fit was evaluated by examining plots of predicted and observed spawner-to-smolt relationships and an analysis of residuals. Pearson residuals (PR), which express the deviation relative to the predicted variability, were computed from:

$$(12) \quad PR_{i,t} = \frac{\log(\hat{R}_{i,t}) - \log(R_{i,t})}{\sigma_i}$$

Residuals were plotted as a function of spawning stock size and brood year to evaluate the functional form of the model (e.g. failure to include depensatory mortality) and non-stationarity, respectively. Quantile-quantile plots were used to determine the extent to which residuals were normally distributed. The standard deviation (SDR) and median of the absolute residuals (MAR) were computed for each population. SDR and MAR should have respective expected values of 1 and 0.67 if residuals are normally distributed.

The χ^2 goodness of fit test statistic was used to test the null hypothesis that the models fit the data. The discrepancy between predicted and observed values was computed as:

$$(13) \quad X^2 = \sum_{i,t} \frac{(\log(R_{i,t}) - \log(\hat{R}_{i,t}))^2}{\log(\hat{R}_{i,t})}$$

X^2 approximates the χ^2 distribution with degrees of freedom = n-1 (Sokal and Rolf 1981). Given n=259 smolt-spawner observations across 17 populations, there is not sufficient evidence to reject the null hypothesis, that is, model fit can be considered adequate, if $X^2 < \chi^2_{.05[258]}$ where $\chi^2_{.05[258]}=221.8$.

Hierarchical BH, LHS, and RI models were compared using the small sample size Akaike Information Criteria (AIC_c , Burnham and Anderson 2002) and the Deviance Information Criteria (DIC, Gelman et al. 2003). Both criteria quantify the tradeoff between model fit and complexity. AIC_c is computed as,

$$(14) \quad AIC_c = -2\log(L(data|\hat{\theta})) + 2K \left[\frac{n}{n-k+1} \right]$$

The first term determines the model deviance computed at the maximum likelihood parameter estimates ($\hat{\theta}$ represents a vector of MLEs for the 55 parameters of the hierarchical model) and the second term represents model complexity based on the number of model parameters (K=55) and sample size (n=259). The model with the lowest AIC_c value is considered to have the best out-of-sample predictive power. More commonly, alternate models are compared based on differences between model-specific AIC_c values (AIC_{c_i}) and the lowest AIC_c value ($AIC_{c_{min}}$) across models ($\Delta_i = AIC_{c_i} - AIC_{c_{min}}$). Δ_i values represent the level of empirical support for each model (Burnham and Anderson 2002):

$\Delta_i < 2 =$ strong

$2 < \Delta_i < 10 =$ considerably less

$\Delta_i > 10$ essentially no support

The likelihood of each model will be proportional to $e^{-0.5\Delta_i}$. Probabilities for each model, termed AIC weights (w_i), were computed by dividing the likelihood of each model by the sum of likelihoods across models:

$$(15) \quad w_i = \frac{e^{-0.5\Delta_i}}{\sum_i e^{-0.5\Delta_i}}$$

When comparing BH, LHS, and RI hierarchical models, the complexity term in the AIC_c formula is constant and Δ_i differences will be determined only by model deviance. That is, models could be compared strictly on differences between their log-likelihood values at their maximum likelihood estimates. AIC is used in this analysis because model support criteria ($\Delta_i < 2$, $2 < \Delta_i < 10$, $\Delta_i > 10$) have been developed within the context of AIC studies (Burnham and Anderson 2002).

The Deviance information criteria (DIC) is a Bayesian analogue of AIC that accounts for uncertainty in parameter estimates and model fit:

$$(16) \quad DIC = -2\log(L(data | \hat{\theta})) = 2\hat{D}_{avg} - D_{\hat{\theta}}$$

where, \hat{D}_{avg} is the average deviance (as defined for eqn. 14) across the posterior sample, and $D_{\hat{\theta}}$ is the expected deviance. There is some debate as to how this latter statistic is computed (Spiegelhalter 2002). In this analysis we approximate $D_{\hat{\theta}}$ based on the minimum deviance across all samples from the joint posterior distribution. The difference between \hat{D}_{avg} and $D_{\hat{\theta}}$ is termed the effective number of parameters (pD). pD approximates the number of ‘unconstrained’ parameters in the model, where a parameter counts as: 1 if it is estimated with no constraints or prior information; 0 if it is fully constrained or all the information about the parameter comes from the prior distribution; or an intermediate value if both the data and prior distributions are informative (Gelman et al. 2003).

2.5 Evaluation of Regional Distributions of Stock-Recruitment Parameters for Simulating Coho Population Dynamics in Georgia Basin West and the Thompson River

We evaluated whether regional distributions of stock-recruitment parameters developed from the hierarchical model would generate trends in aggregate escapements in the Georgia Basin West management unit and the Thompson River that are consistent with observations. This required a synthesis of GIS data to estimate freshwater habitat capacity in these regions (2.5.1), compilation of historical harvest rate, marine survival

rate, and escapement data (2.5.2), and simulation of historical aggregate escapement trends (2.5.3).

2.5.1 *Freshwater Habitat*

The BC Watershed Atlas (WA) provides a digital inventory of all blue lines that are drawn on NTS 1:50,000 scale maps. The WA contains a “Historical Fish Distribution” layer (ftp://fshftp.env.gov.bc.ca/pub/outgoing/bc50kfiss/hist_fish_dist/shapefiles) that defines the upstream limit for anadromous salmonids. These limits were determined based on observed fish presence and known barriers as recorded in the FISS database updated to the year 2000. We extracted all stream reaches from the fish distribution layer that were accessible to anadromous salmonids within Georgian Basin West and Interior Fraser management units. Streams outside of the Thompson River drainage were excluded because the abundance of mid- and upper-Fraser coho populations is very likely not limited by habitat (J. Irvine and M. Bradford, Fisheries and Oceans Canada, pers. comm.). Thus, application of a simple habitat-based model will substantially overestimate the true capacity of these streams. As well, the status of coho populations in the Thompson drainage is the most important conservation issue for south coast coho and it is therefore reasonable to focus the analysis in this area. The sum of accessible stream length from the Watershed Atlas was used to determine the number of km of freshwater rearing habitat for coho salmon in GBW and the Thompson River Drainage.

2.5.2 *Escapement, Harvest Rate, and Marine Survival Trends*

The sum of annual escapements from all streams that are surveyed in GBW and the Thompson drainage was computed from SEDS records to produce aggregate escapement trends. SEDS contained escapement data from 97 streams in GBW and 87 streams in the Thompson River drainage. For the Thompson, we used the same escapement data compiled in Folkes et al. (2005), while data from GBW was obtained directly from the SEDS database. The Thompson escapement time series excludes hatchery contributions but data were not available to do this for GBW populations.

We used annual marine survival rates determined from CWT returns estimated from previous analyses. An aggregate marine survival rate for GBW populations for brood years 1972-2001 was computed by averaging the rates from index stocks (Big Qualicum, Quinsam, and Black) reported in Simpson et al. (2004). We used the marine

survival rates for brood years 1987 to 2001 from enhanced coho releases in Eagle and Salmon Rivers, and Louis, Lemieux, and Spius Creeks (Irvine et al. 2001) as a surrogate for the survival rate of wild stocks in the Thompson drainage. A linear relationship between marine survival rates for the Thompson and GBW index stocks was computed ($n=15$, $r^2=0.39$, $m_{\text{Thompson}}=0.0059+0.5004*m_{\text{GBW}}$). Survival rates for the Thompson aggregate from brood years 1972-1986 were predicted by substituting GBW survival rates into the linear regression. We used historical harvest rates reported in Table 3 of Folkes et al. (2005) and Simpson et al. (2004) for the historical trends in exploitation rates for the Thompson and GBW aggregates, respectively.

2.5.3 *Simulation of Aggregate Escapement Trend*

The trend in the aggregate escapement for GBW and the Thompson River drainage between 1975 and 2004 was simulated as follows:

- 1) A random draw from the predictive marginal distributions of stock productivity and carrying capacity were used to determine stock-recruitment parameters for each population in the GBW or the Thompson drainage. The number of populations is uncertain, so both low (10) and high (90) values were simulated.
- 2) The mean number of smolts produced for each population per unit stream length was calculated from the LHS stock-recruitment model for each timestep using the escapement 2 years earlier. The mean smolt number was multiplied by a lognormal random deviate (with SD = mean value from the hierarchical meta-analysis of 0.36) to simulate variation in freshwater survival rate.
- 3) The number of returning spawners per unit stream length was computed based on the product of the smolt production from the previous year, and the historical marine survival rate and the proportion of fish surviving harvest (1-historical harvest rate) for the return year.
- 4) The escapement in each year for GBW or the Thompson drainage was computed as the product of the sum of populations-specific escapements and the number of km of stream length per population. The latter value was simply the ratio of the total number of km of accessible habitat divided by the number of populations that were simulated.

The average observed escapement over the first 3 years, divided by the number of populations, was used to initialize the simulations. The procedure was repeated 500

times, and the distribution of aggregate annual escapements across trials was plotted over time and compared to the observed aggregate escapement trend.

3.0 Results

3.1 Model Fit and Comparison

Independent and hierarchical fits of the Beverton-Holt (BH), Logistic Hockey Stick (LHS), and Ricker (RI) models are shown in Figures 1-3, respectively. As expected, the BH model fitted independently to each population (the non-hierarchical model) produced unrealistically high stock productivity estimates in cases where there was little decline in smolt production at low stock size (e.g. Big Qualicum, Bingham, Hooknose, and Minter populations). The hierarchical version of the BH model provided more realistic estimates of stock productivity in these cases because estimates were strongly influenced by the regional distribution, which was mostly determined based on stock productivities from populations where it was better defined. The independently estimated LHS and RI models did not predict very high stock productivities for stocks that were problematic using the BH model (Fig. 's 2 and 3). The increased structural rigidity of the LHS model imposed by the tuning parameter was helpful in these circumstances. The RI model predicted strong overcompensation for many of the populations even though there was little data to suggest that smolt production declines at higher escapements (Fig. 3). This behaviour was most apparent for stocks where independently fitted stock productivity estimates under the BH model were very high. In cases where there is little decline in recruitment at low stock size, the BH model estimates unrealistically high stock productivity, while the Ricker model estimates lower productivity by overestimating of the strength of density dependence. The LHS model avoids both these pitfalls.

Parameters defining regional distributions of stock productivity and carrying capacity varied considerably between stock-recruitment models (Table 3). Estimates of the mean stock productivity were highest for the BH model ($\mu_{\alpha}=86$ smolts/spawner) and lowest for the RI model ($\mu_{\alpha}=43$ smolts/spawner). The across-population variance in stock productivity was considerably lower for the BH model ($CV_{\alpha}=0.18$) compared to the other models ($CV_{\alpha}=0.36-0.39$), although variance in carrying capacity was similar ($CV_{\beta}=0.57-$

0.59). The BH and RI models predicted higher smolt carrying capacities ($\mu_{\beta}=1397$ and 1357 smolts/km) than the LHS model ($\mu_{\beta}=1154$ smolts/km).

All hierarchical models fit the data well. X^2 statistics for the BH (6.98), LHS (6.23), and RI (7.13) models were well below the $\chi^2_{.05[258]}$ threshold of 221.8. Thus, there was not sufficient evidence to reject the null hypothesis that the models fit the data and model fit can be considered adequate in all cases. The structural forms of all stock-recruitment models were consistent with the assumption that residuals are log normally distributed. The standard deviation of Pearson residuals for all populations was very close to 1 and the median absolute values of residuals were just above the expected value of 0.67 (Table 4). Residual patterns were very similar for all hierarchical models so results for only the LHS model are shown. There was no apparent trend of higher positive residuals (over-predictions of smolt numbers) at low stock size that would be indicative of compensatory mortality (Fig. 4). Most populations did not show any temporal trend in residuals with the exception of Carnation Creek and Skagit River, where the model underpredicts smolt production since the mid 1990's (Fig. 5). Consistent with SDNR and MAR statistics, quantile-quantile plots showed that residuals were normally distributed, although there was evidence for modest overdispersion in the Snow Creek data (Fig. 6).

There was no relationship between maximum likelihood estimates of stock-productivity and smolt carrying capacity estimates across populations for both hierarchical and non-hierarchical models (Fig. 7). As reported in many stock-recruitment analyses (e.g. Chen and Holtby 2002), there was strong covariation among parameter estimates within stocks (Table 5). Parameters were negatively correlated in the case of BH and LHS models, implying that a stock could be more productive with lower capacity, or visa-versa. The extent of parameter confounding varied among models and was higher for the Beverton-Holt model due to its ability to predict large asymptotic carrying capacity in cases where capacity is poorly defined from the data (e.g. Big Beef or Deschutes in Fig. 1). Parameters tended to be positively related in the case of the Ricker model, with higher estimates of productivity generating a higher peak in recruitment, which also implied greater density-dependent mortality.

There was essentially no support for the Ricker stock-recruitment model based on both AIC_c and DIC criteria (Table 6). The BH model was highly unstable. Convergence

could only be obtained by reducing the variance of the prior on stock-specific productivity from $CV_{\alpha_i}=10$ to $CV_{\alpha_i}=1$ (Table 2). The AIC results strongly suggest that the LHS model will provide the best out-of-sample predictive power relative to either BH or RI models. The DIC results also support the LHS model although it indicates moderate support for the BH model. However for the DIC comparison, the BH model required use of a weak prior on stock productivity. In the case of the AIC_c criterion, all models have the same number of parameters but the LHS model fits the data best. The hierarchical models have fewer effective parameters than the total number of parameters ($K=55$) because the hyper distributions constraint population-specific estimates in the cases where they are poorly defined. The LHS model has the fewest number of effective parameters because it has a more rigid structure compared to other models. The Beverton-Holt model appears to have similar rigidity compared to the LHS model, but some of this is caused by the use of a weak prior on α_i to meet convergence criteria.

3.2 Regional Distributions of Stock-Recruitment Parameters and Sustainable Harvest Rates

Prior probabilities for the means of regional distributions of stock productivity and carrying capacity were very uninformative (Table 2, Fig. 8a and b) and had no influence on the resulting maximum likelihood estimates of hyper-parameters. However, in the absence of a weakly informative prior on the lower limit of across-population variation in stock productivity and carrying capacity, the hierarchical model would estimate an unrealistically low variance for one of the two parameters (CV_{α} or CV_{β}) by inflating the variance estimate for the other parameter. Values for the variance of the inverse gamma distribution ($\mu(CV_x)$ and $\tau(CV_x)$ in Table 2) defining the prior for hyper-parameter variances were chosen to create a steep probability gradient at very low variance estimates (Fig. 8c and d). The low precision of the prior distributions ($\tau(CV_x)=0.2$) resulted in a very flat log probability surface except at very low variance estimates (e.g. $CV_{\alpha}<0.25$ in Fig. 8c). The mean for the prior ($\mu(CV_x)$) had a minor influence on hyper variance estimates. The maximum likelihood estimates of CV_{α} ranged from 0.33-0.44 for the LHS model as $\mu(CV_x)$ was increased from 0.05-1.6. The influence of the prior was weak because there was a reasonable amount of information in the data about the variances of the hyper-distributions.

The underlying stock-recruitment function had a significant influence on the regional distributions of stock productivity and carrying capacity (Fig. 9). The LHS model resulted in the lowest mean carrying capacity and an intermediate mean stock productivity relative to the BH and RI models. Uncertainty in the hyper-parameters defining regional distributions of stock productivity and carrying capacity was moderate (Fig. 10). 50% of the posterior samples for the mean and CV of stock productivity for the LHS model fell between 58-67 smolts/spawner and 0.48-0.65, respectively. 50% of the posterior samples for the mean and CV of carrying capacity fell between 1144-1432 smolts/km and 0.56-0.72, respectively. There was no correlation between hyper-distribution parameters.

The predictive marginal posterior distributions of stock-recruitment parameters based on the hierarchical LHS model are shown in Figure 11. The means and medians of the marginal distributions for stock productivity and carrying capacity were 79 and 65 smolts/spawner and 1642 and 1292 smolts/km, respectively. The marginal predictive distribution for carrying capacity was similar to the most likely estimate for the regional distribution although the former provides a better approximation to the distribution of capacities from the extensive database compiled by Bradford et al. (1999). The marginal predictive distribution for stock productivity was considerably more variable than the most likely regional distribution.

Distributions of harvest rate (U_{msy}) and spawner densities (S_{msy}) that result in maximum sustainable yields based on samples from the marginal predictive distributions are shown in Figure 12. As expected, U_{msy} declines considerably at lower marine survival. In the worst scenario (marine survival = 0.025), 20% of the populations are unsustainable even in the absence of harvest. Modal U_{msy} values at $ms=0.025$, 0.05, and 0.10 were 0.3, 0.6, and 0.7, respectively. Escapement to achieve MSY increased at higher marine survival rates. U_{msy} predictive distributions varied considerably among stock-recruitment models (Fig. 13). At low marine survival ($ms=0.025$), the Beverton-Holt model suggests a much higher U_{msy} relative to the other models because it predicts higher stock productivity (Fig. 9). U_{msy} distributions for Beverton-Holt and logistic hockey stick models were similar at marine survival rates of 0.05 and 0.1. The Ricker model consistently predicted the most conservative U_{msy} distributions.

3.3 Evaluation of Regional Distributions for Georgia Basin West and Thompson River Coho Aggregates

There were a total of 1,335 and 2,268 km of accessible stream length distributed over 245 and 118 streams in the Georgia Basin West management unit and the Thompson River, respectively (Table 7, Fig. 14). The product of total stream length and the mean of the marginal distribution for carrying capacity (Fig. 11, 1642 smolts/km) predicted total freshwater capacities for GBW and the Thompson of 2.2 and 3.7 million smolts, respectively (Table 8). The adult capacity for GBW and the Thompson River could be as low as 54,000 and 93,000 at a marine survival rate of 2.5%, and as high as 220,000 and 372,000 at a marine survival rate of 10%, respectively. We backcalculated historical adult recruitments based on annual escapements and exploitation rates. Historical GBW and Thompson River recruitments were 334,000 and 95,000 between 1975 and 2004. The GBW recruitment, which occurred over a period when marine survival rate averaged 8.2%, was considerably higher than adult carrying capacity of 219,000 spawners estimated from the product of habitat and smolt carrying capacity at a similar marine survival rate (10%). In contrast, the Thompson River historical recruitment of 95,000 (average marine survival =4.7%) was ½ the capacity-based recruitment estimate of 186,000 at a marine survival of 5%. It is possible we have overestimated the amount of stream length that contributes to coho production by including higher order mainstem reaches in the total. Removing 6th and 7th order systems (mainstem Lower Thompson, North Thompson, and Adams) reduced accessible stream length by approximately 50% (Table 8) and lead to good agreement between observed and historical recruitments.

Marine survival rates for both GBW and Thompson populations were very high in the mid 1970's and relatively good until the early 1990's (Fig. 15). GBW survival rates declined steadily over the 1990's reaching a minimum of 1.5% in 2000. Thompson River survival rates also declined over this period. GBW survival rates were 1.8-fold greater than Thompson River survival rates between 1987 and 1994, but have been similar since then. Historical exploitation rates of GBW and Thompson populations were very similar and averaged about 70% prior to the fisheries closure in 1995. The Thompson River aggregate escapement trend was relatively constant at a average of 45,000 spawners between 1975 and 1989, after which it dropped substantially, reaching a minimum of

about 6,000 spawners in 1996 (Fig. 16). The aggregate escapement trend for GBW was relatively stable and did not show a decline in abundance that would be expected based on the declining trend in marine survival rates. Reductions in harvest beginning in the 1995 would have partially offset the effects of reduced marine survival, but it was surprising that escapements did not decline in the 1980's when marine survival declined and exploitation rates remained high. We suspect that the GBW escapement data may not accurately reflect the escapement of wild populations because it includes hatchery contributions, which substantially increased over this period. Increased monitoring effort in the latter part of the time series could also have masked declines in wild populations.

The trend in across-trial medians of simulated escapement provided a reasonable match to the observed escapement trend for the Thompson aggregate, although the model tended to underpredict escapement in most years (Fig. 16). This may seem surprising as the simulations were based on 2268 km of habitat that overpredicted the backcalculated recruitment by 2-fold in the static analysis (Table 8). The simulations underpredicted the aggregate escapement because many of the simulated populations were overexploited, and very low marine survival rates after the fisheries closure in 1995 did not allow the populations to rebuild. There was less correspondence between predicted and observed aggregate escapements in GBW. The model predicted a very large drop in escapement at the start of the time series due to very high exploitation rates (92% in 1976), but this change was not seen in the SEDS data. The model predicted fairly stable escapement for much of the time series similar to the observed escapement trend, but the predicted escapement was about 4-fold lower than what was observed. Part of this discrepancy could be due to underestimating carrying capacity for GBW (Table 8) assuming the escapement data reflects the abundance of wild populations. However, this bias does not explain all of the discrepancy. Similar to the dynamic for the Thompson aggregate, part of the discrepancy in simulated and observed aggregate escapements for GBW resulted from overexploitation of weak stocks, and very poor marine survival late in the time series that did not allow the populations to recover after the fisheries closure.

The extent of variation around predicted annual aggregate escapements depended on the number of populations that were simulated. When only 10 populations were simulated (Fig. 16a) there was considerably more inter-trial variance because the

probability of randomly selecting an unrepresentative sample of high or low stock productivities and carrying capacities from the regional distributions increased. Simulating more populations (e.g. 90 in Fig. 16b) provided a representative sample from the marginal distributions of stock-recruitment parameters resulting in similar aggregate trends across trials.

4.0 Discussion

The Logistic Hockey Stick model provided the best fit to the coho salmon spawner-to-smolt data and was selected as the best model based on AIC and DIC criteria (Table 6). The Ricker model provided the poorest fit to the data and the BH model was highly unstable. In cases where there is little information about recruitment at low stock size, the Ricker model predicted much lower stock productivity compared to Beverton Holt or LHS models (Table 3) by increasing the magnitude of compensatory effects (Fig. 3). The increased flexibility of the Ricker model in such cases was not justified based on the data as evidenced by its higher AIC and DIC statistics. Prediction of strong overcompensation is also not consistent with current understanding of coho recruitment dynamics (Bradford et al. 2000, Barrowman et al. 2003). This analysis supports the use of the LHS model to predict smolt production for coho salmon.

The hierarchical Logistic Hockey Stick model predicted an expected freshwater stock productivity for coho salmon of approximately 60 smolts/spawner (Table 3). This is considerably less than a productivity of 80 smolts/spawner calculated from the average of independent estimates for each population (Bradford et al. 2000). The 33% difference is consistent with previously reported biases in regional distributions that can occur by not using a hierarchical model (Chen and Holtby 2002, Barrowman et al. 2003). For example, Chen and Holtby (2002) showed that the means of regional distributions of stock productivity based on independently derived estimates for coho salmon were between 20% (Thompson River) and 54% (North Coast) higher than those derived from a hierarchical analysis. The hierarchical model structure reduces the effects of poorly defined stock-specific productivity estimates on the regional distribution. Chen and Holtby estimated 6.5 adult recruits/spawner for Thompson River coho salmon populations using SEDS data. This converts to approximately 65 smolts/spawner

assuming an average marine survival rate over their period of record (1975-99) of 0.1 (Fig. 1c, Bradford et al. 2000), virtually the same mean estimated in this analysis.

In this analysis, as in Chen and Holtby's (2002, Fig. 4c and g), there was strong covariation in parameter estimates within a stock (Table 4). This covariation occurred because the data was not informative enough in some cases to distinguish whether a population was large and unproductive or visa-versa. The extent of parameter confounding we observed depended on the form of the stock-recruitment model. The LHS model showed less parameter confounding than the BH model because of its more rigid structure. Estimates of parameter confounding under the Ricker model provided here are lower than reported in Chen and Holby (2002). This occurred because of different model parameterizations, but also because the spawner-to-smolt data used in this analysis has considerably less observation error than the spawner-to-adult recruit data generated from the SEDS database. Much of the parameter covariation reported by Chen and Holtby likely came from high observation error. There was no evidence of covariation between stock productivity and carrying capacity among populations based on both hierarchical and independent stock-recruitment analyses (Fig. 7). Evidence for within-stock covariation (Table 5 or Fig. 4c and g of Chen and Holtby 2002) in no way implies that there is strong covariation in parameters across stocks.

Predicted regional distributions of stock productivity (Fig. 11) were used to define distributions of harvest rates that attain maximum sustainable yields (Umsy). Marine survival rate for index stocks from the Georgia Basin West MU since 1996 (brood years 1996-2001) have averaged 2.1%. Under these conditions, a harvest rate as low as 20% is not sustainable for at least half of the populations modeled by the regional distribution (Fig. 12). Much higher harvest rates could be supported under improved marine survival, but only for a fraction of the populations. For example, at an improved survival rate of 5%, about 1/3rd of the populations could sustain a harvest rate of 60%, but this rate would not be sustainable for the majority of populations. At low (2.5%) and moderate (5%) marine survival regimes the LHS model is more conservative or equivalent to the Beverton-Holt model, respectively (Fig. 13). The Ricker model predicted the most conservative distribution but this model, and the Beverton-Holt model, had weaker out-of-sample predictive power compared to the Logistic Hockey Stick model. Thus, the

regional distribution of Umsy based on the LHS model is the most defensible distribution to use for policy analysis. Predictive marginal distributions of stock productivity and carrying capacity from the LHS model will be used in a forthcoming analysis that evaluates alternate harvest strategies based on both catch and conservation criteria.

Adult carrying capacity predicted by the product of the mean of the marginal distribution of smolt capacity and accessible stream length was different than backcalculated estimates derived from historical escapements and harvest and marine survival rates. The model underpredicted adult carrying capacity by about 2-fold for GBW and overestimated capacity by a similar magnitude for the Thompson River drainage. In the case of the Thompson, it is possible that the total amount of stream length used for coho rearing was overestimated because larger mainstem reaches, which may only be used as migratory pathways, comprised about 50% of the total. There was good agreement between predicted and backcalculated carrying capacity when these reaches were removed from the calculations. There are two possible reasons why the backcalculated recruitment to GBW appears to be so much higher than the habitat-based estimate. First, accessible stream length could be underestimated as many productive side-channel habitats would not be shown on a 1-50,000 map-scale. Alternately, the habitat model may be correct and backcalculated capacity could be overestimated because escapement data included hatchery contributions. In the absence of reliable estimate of naturally produced escapement for GBW, the comparison of predicted and 'observed' carrying capacities for GBW remains very inconclusive.

The simulated aggregate escapements for GBW and the Thompson River, that were driven by historical exploitation and marine survival rates and random draws from the marginal distributions of stock-recruitment parameters underpredicted the observed escapements. The simulations also tended to overpredict the extent of population decline due to the combination of overexploitation and reduced marine survival. The datasets used to develop the marginal distributions of stock-recruitment parameters were from index streams. It has been suggested that index streams may be more productive than the average stream, as unproductive systems with few or erratic numbers of fish are difficult to justify monitoring (Bradford et al. 2000). Our analysis suggests that this is not the case with respect to populations in the GBW management unit or the Thompson River. The

distributions of stock-recruitment parameters generated from the index stream data tended to predict a decline in populations that was more severe than what the escapement data suggests. This conclusion should be considered very preliminary as marine survival and exploitation rates for Thompson populations are highly uncertain, and the GBW escapement data likely contains temporally varying and large hatchery contributions. However, given uncertainties in the data and the conservative nature of model predictions to harvest, it seems reasonable to use the regional distributions of carrying capacity and stock productivity developed from the hierarchical meta-analysis to represent the population dynamics for GBW and Thompson River stocks in the forthcoming harvest rate analysis.

Acknowledgements

Thanks to Blair Holtby, Mike Bradford, Michael Folkes, Jim Irvine, Michael Chamberlain, Kent Simpson, Eric Parkinson, Joseph Tadey, Gary Morishima, and Bob Hayman for providing data or useful commentary on this analysis.

5.0 References

- Barrowman, N.J., and R.A. Myers. 2000. Still more spawner-recruitment curves: the hockey stick and its generalizations. *Can. J. Fish. Aquat. Sci.* 57:665-676.
- Barrowman, N.J., Myers, R.A., Hilborn, R., Kehler, D.G., and C.A. Field. 2003. The variability among populations of coho salmon in the maximum reproductive rate and depensation. *Ecological Applications* 13(3):784-793.
- Bradford, M.J., Myers, R.A., and J.R. Irvine. 2000. Reference points for coho salmon (*Oncorhynchus kisutch*) harvest rates and escapement goals based on freshwater production. *Can. J. Fish. Aquat. Sci.* 57: 677-686.
- Bradford, M.J., Korman, J., and P.S. Higgins. 2005. Using confidence intervals to estimate the response of salmon populations (*Oncorhynchus* spp.) to experimental habitat alterations. *Can. J. Fish. Aquat. Sci.* 62:2716-2726.
- Burnham, K.P., and D.R. Anderson. 2002. *Model Selection and Multimodel Inference*, 2nd ed. (Springer).
- Chen, D.G., and L.B. Holtby. 2002. A regional meta-model for stock-recruitment analysis using an empirical Bayesian approach. *Can. J. Fish. Aquat. Sci.* 59: 1503-1514.
- Folkes, M., Ionson, B., and J.R. Irvine. 2005. Scientific advice for input to the Allowable Harm Assessment for Interior Fraser Coho Salmon. Canadian Science Advisory Secretariat Research Document 2005/093.
- Gelman, A., Carlin, J.B. Stern, H.S., and D.B. Rubin. 2003. *Bayesian data analysis*. Chapman and Hall/CRC. 668 pp.
- Hilborn, R. and C.J. Walters. 1992. *Quantitative fisheries stock assessment*. Chapman and Hall, New York, NY.
- Irvine, J.R., C.K. Parken, D.G. Chen, J. Candy, T. Ming, J. Supernault, W. Shaw, and R.E. Bailey. 2001. CSAS Research Document 2001/083.
- McAllister, M.K., Hill, S.L., Agner, D.J., Kirkwood, G.P., and J.R. Beddington. 2004. A Bayesian hierarchical formulation of the De Lury stock assessment model for abundance estimation of Falkland Islands' squid (*Loligo gahi*). *Can. J. Fish. Aquat. Sci.* 61:1048-1059.
- PSC (Pacific Salmon Commission). 2004. *Pacific Salmon Treaty*, March 2004. 116 pp.

- Sharma, R., and R. Hilborn. 2001. Empirical relationships between watershed characteristics and coho salmon (*Oncorhynchus kisutch*) smolt abundance in 14 western Washington streams. *Can. J. Fish. Aquat. Sci.* 58:1453-1463.
- Simpson, K., Chamberlain, M., Fagan, J., Tanasichuk, R.W., and D. Dobson. 2004. Forecast for southern and central British Columbia coho salmon in 2004. Canadian Science Advisory Secretariat Research Document 2004/135.
- Spiegelhalter, D.J., Best, N.G., Carlin, B.P., and A. van der Linde. 2002. Bayesian measures of model complexity and fit. *J. Roy. Stat. Soc. (B)* 64:583-639.
- Sokal, R.R., and F.J. Rohlf. 1981. *Biometry*. W.H. Freeman and Company. New York. 859 pp.

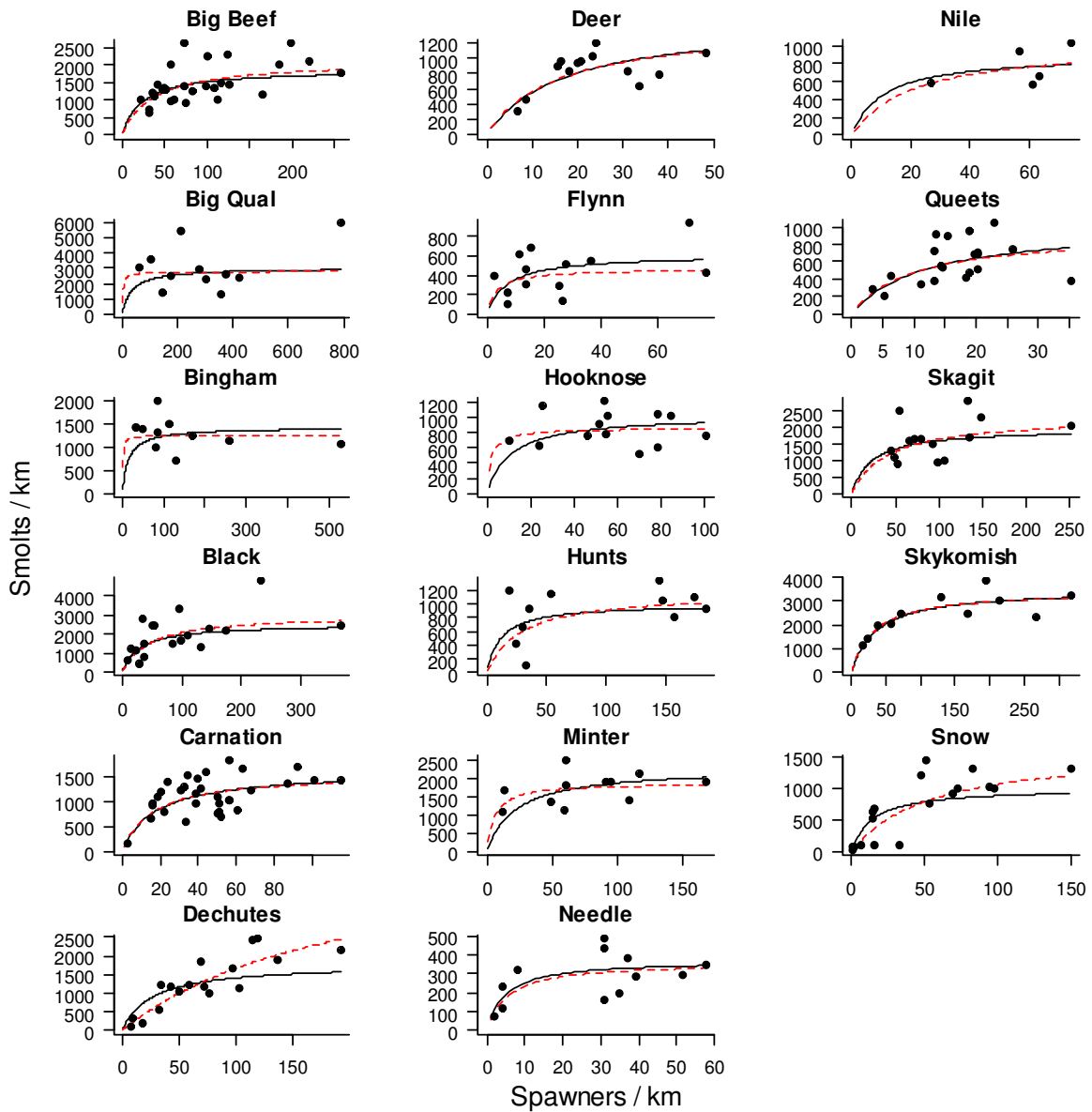


Figure 1. Most likely fits to spawner-to-smolt data for 17 populations based on hierarchical (black solid line) and independently estimated (red-dashed lines) Beverton-Holt stock-recruitment models.

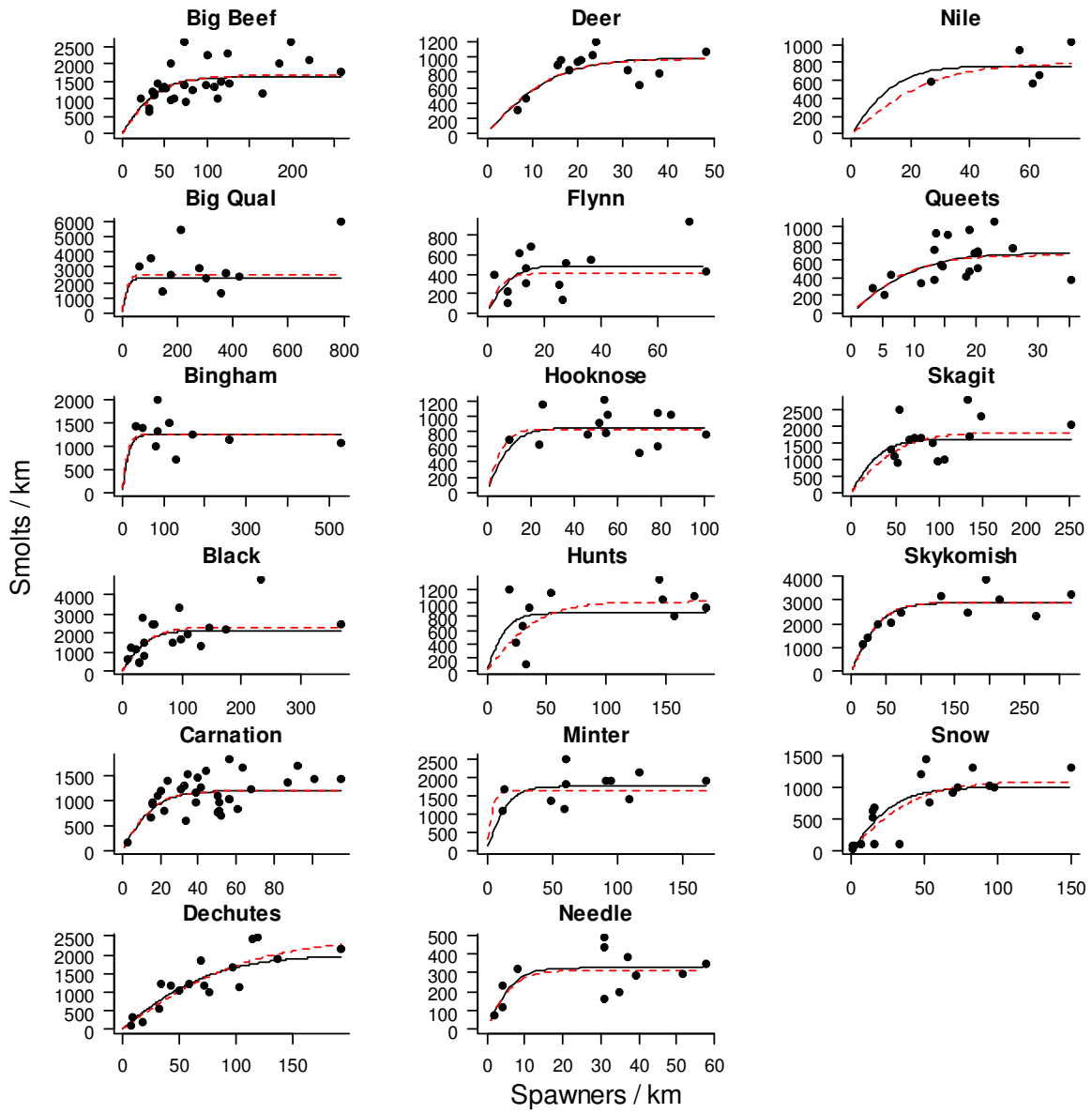


Figure 2. Most likely fits to spawner-to-smolt data for 17 populations based on hierarchical (black solid line) and independently estimated (red-dashed lines) Logistic Hockey Stick stock-recruitment models.

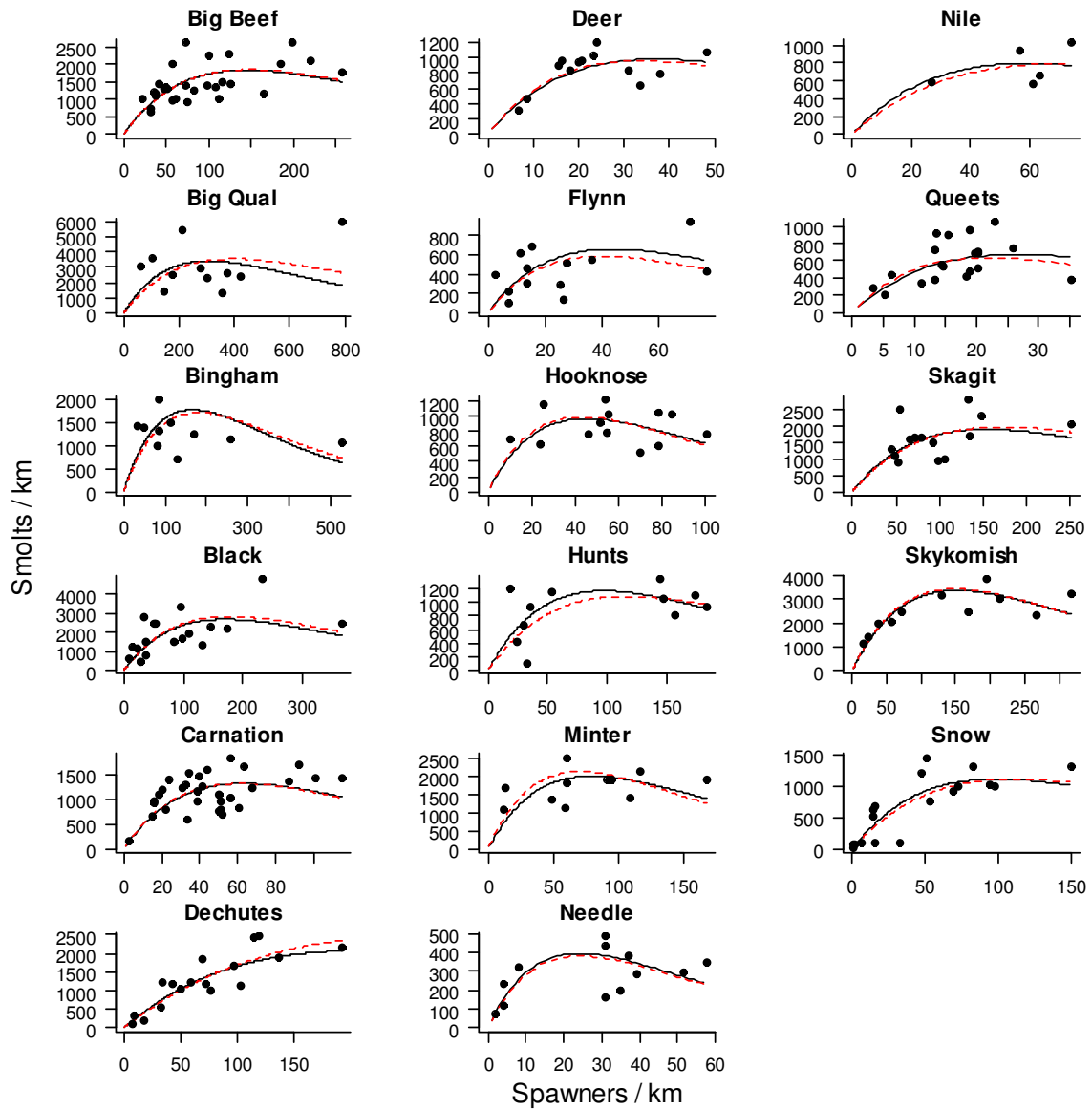


Figure 3. Most likely fits to spawner-to-smolt data for 17 populations based on hierarchical (black solid line) and independently estimated (red-dashed lines) Ricker stock-recruitment models.

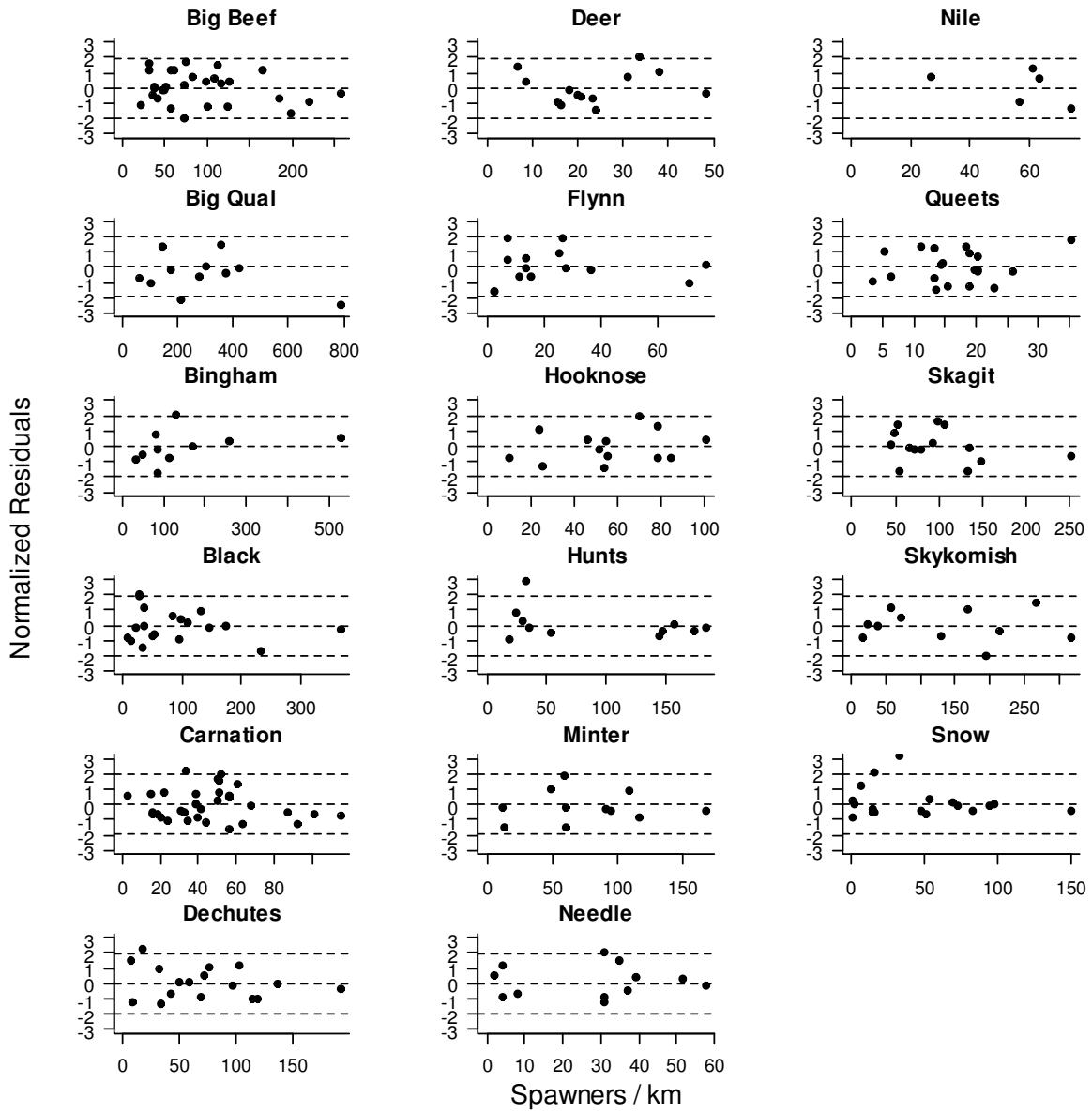


Figure 4. Pearson-residuals from the hierarchical Logistic Hockey Stick model as a function of stock size (spawners/km). The horizontal lines show the median ($y=0$), and 95% confidence intervals ($y=\pm 1.96$). A positive residual indicates that the model overestimates the number of smolts.

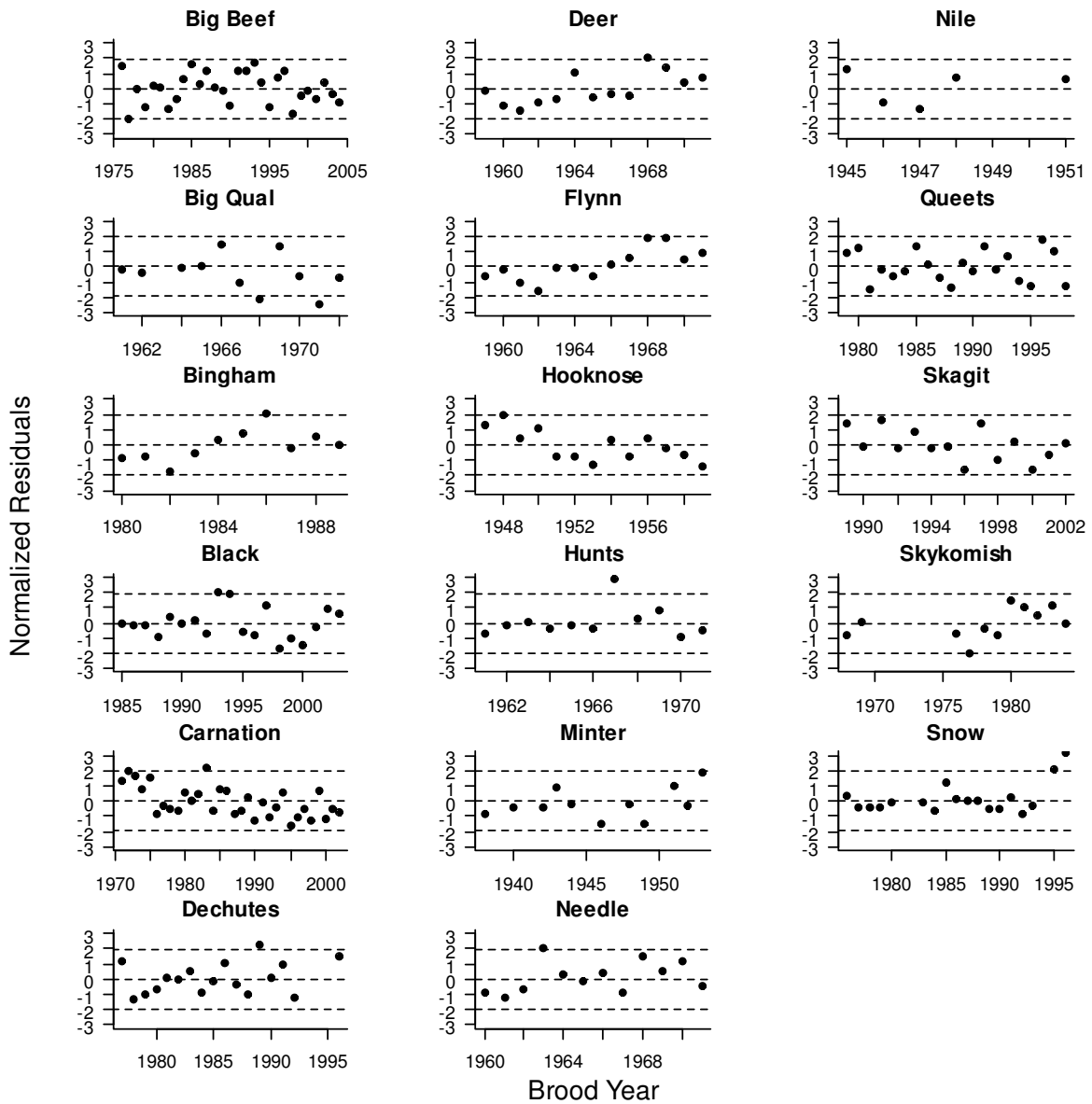


Figure 5. Pearson-residuals from the hierarchical Logistic Hockey Stick model by brood year. The horizontal lines show the median ($y=0$), and 95% confidence intervals ($y=\pm 1.96$). A positive residual indicates that the model overestimates the number of smolts.

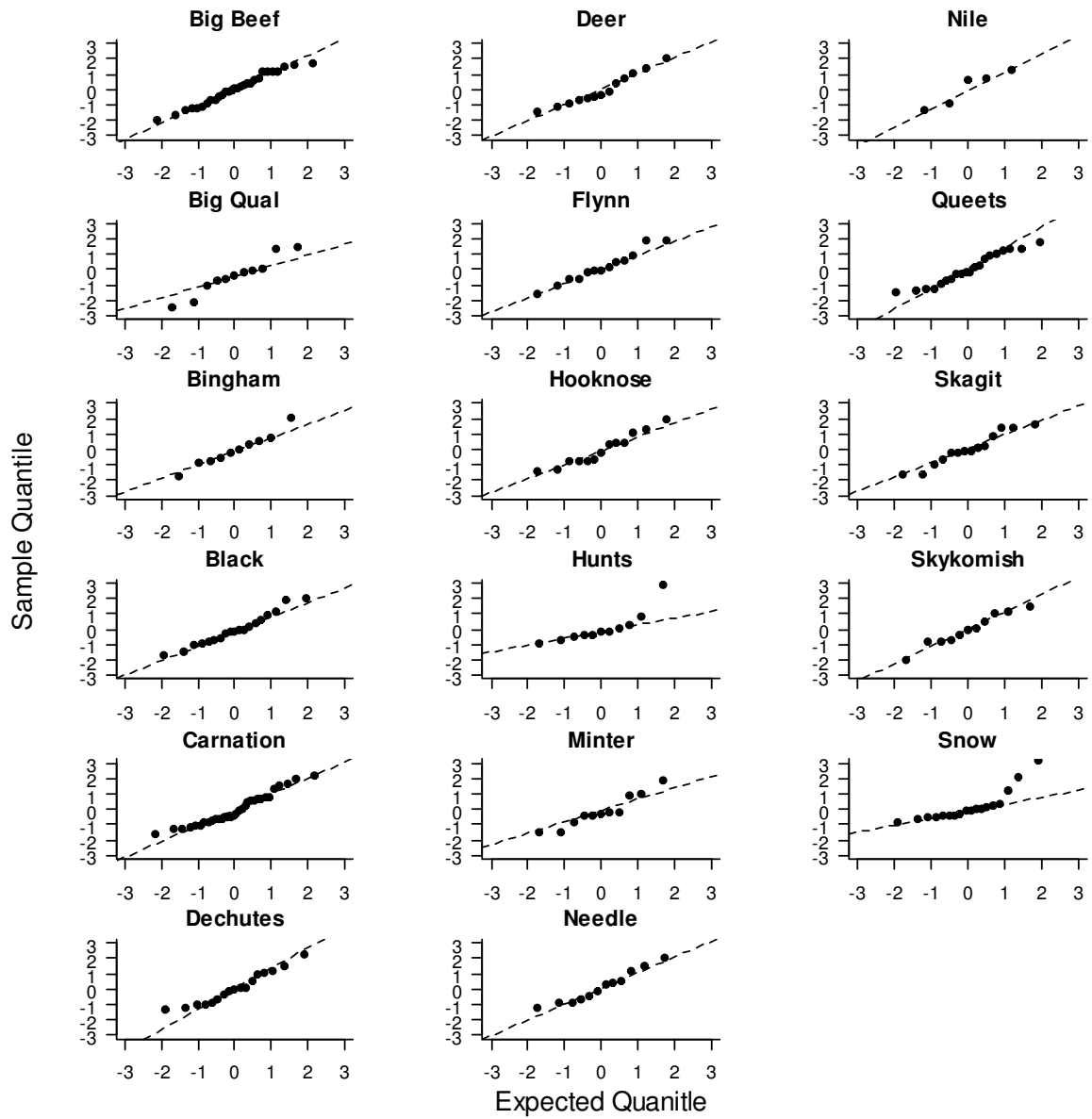


Figure 6. Normal-quantile plots for residuals from the hierarchical Logistic Hockey Stick model.

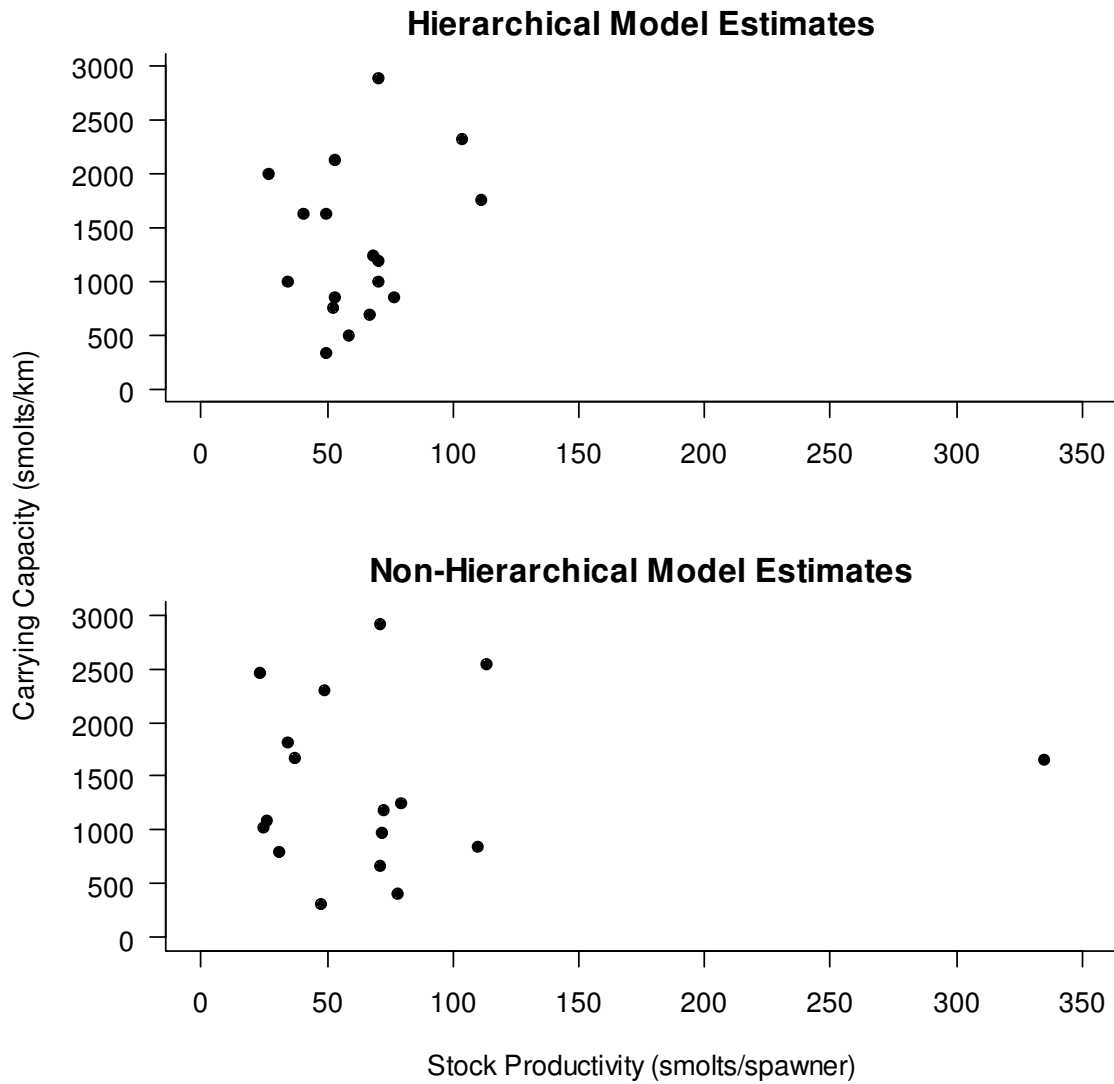


Figure 7. Most-likely estimates of stock productivity and carrying capacity for 17 populations based on the hierarchical and non-hierarchical (independently estimated) Logistic Hockey Stick models.

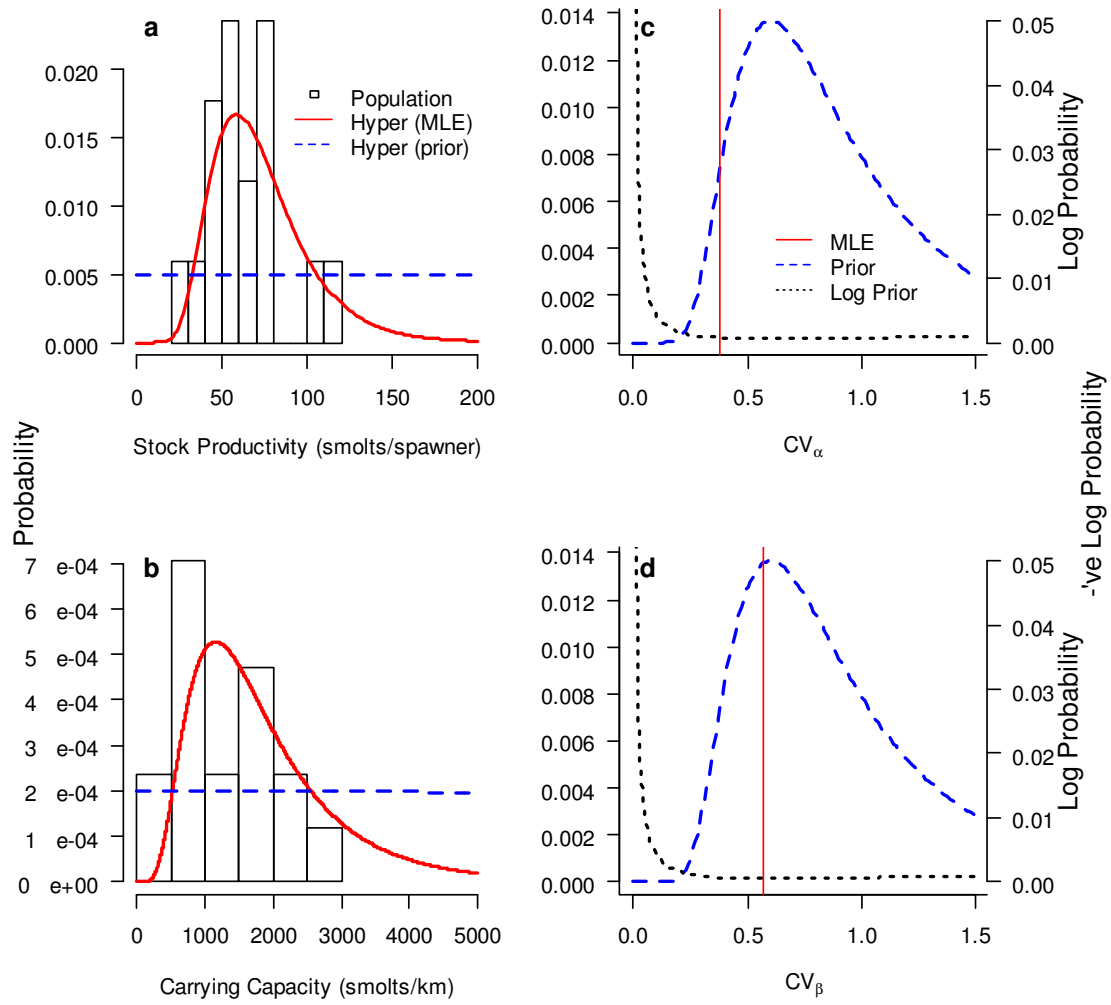


Figure 8. Prior and most likely estimates of the regional distributions for stock productivity (a) and carrying capacity (b) and population-specific estimates for the hierarchical Logistic Hockey Stick model. The prior distribution for the relative variation (CV_α and CV_β) in regional distributions, and the most likely estimate (vertical red line) for stock productivity (c) and carrying capacity (d) are also shown.

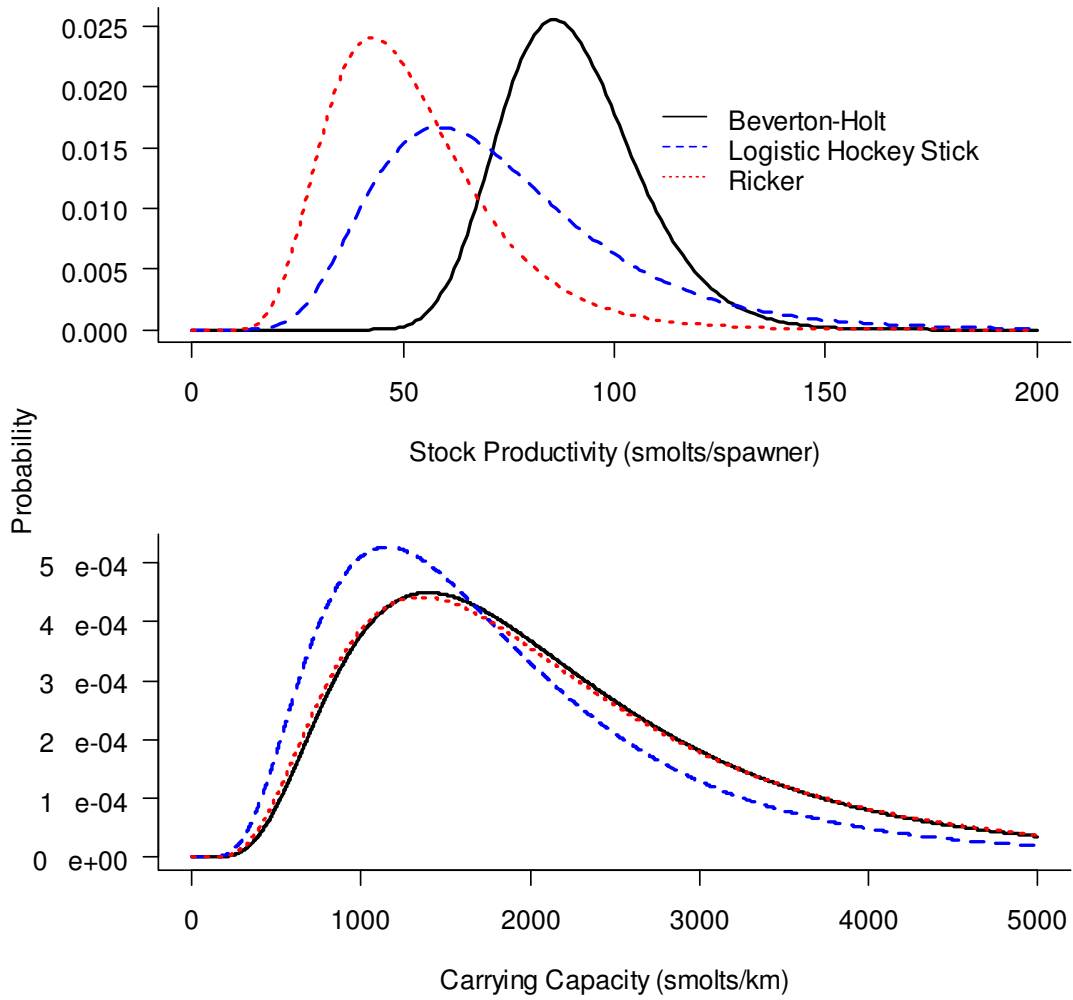


Figure 9. Comparison of most likely estimates of regional distributions for stock productivity and carrying capacity across 3 hierarchical models.

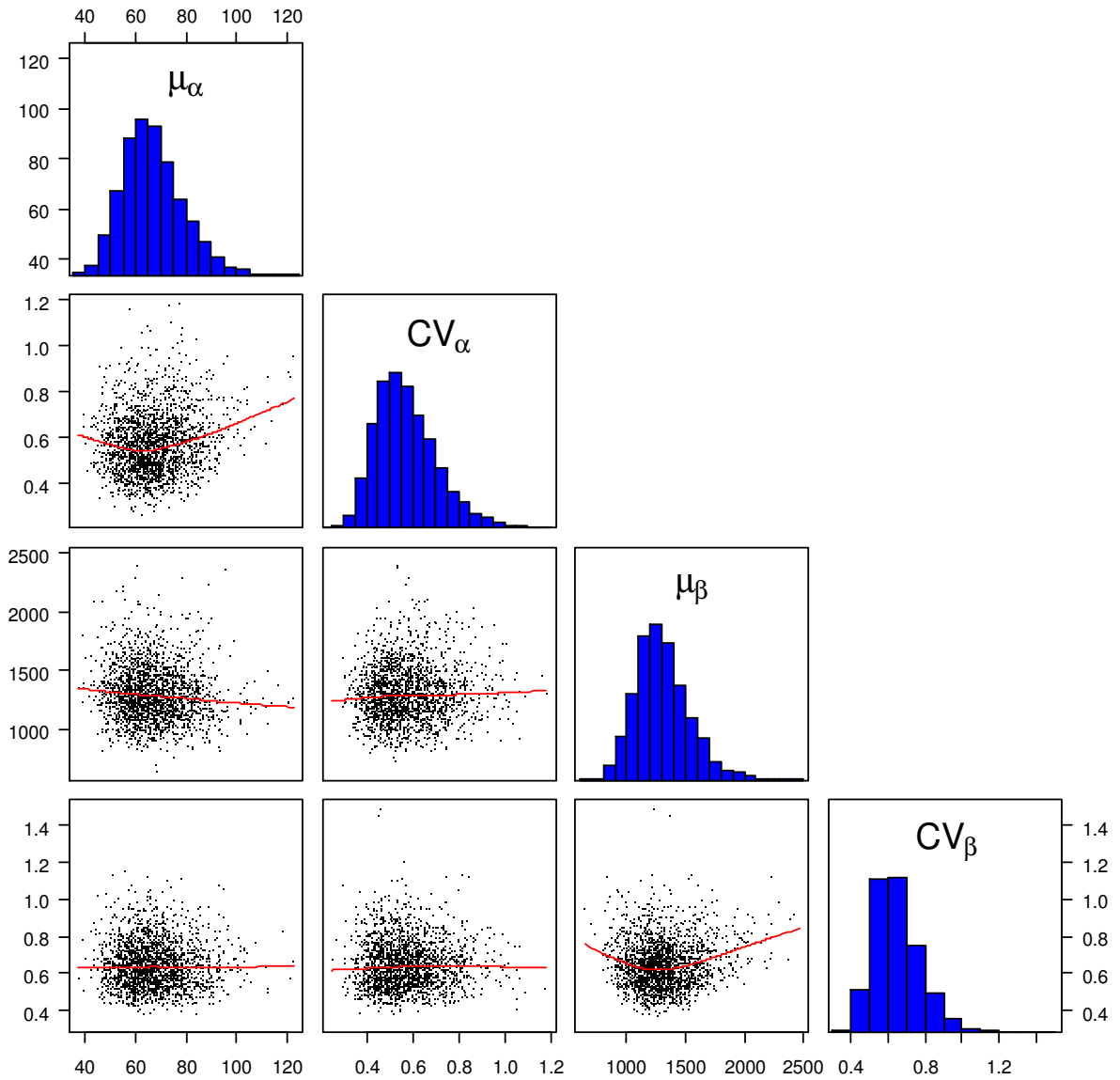


Figure 10. Posterior distributions of regional stock productivity and carrying capacity parameters from the hierarchical Logistic Hockey Stick model.

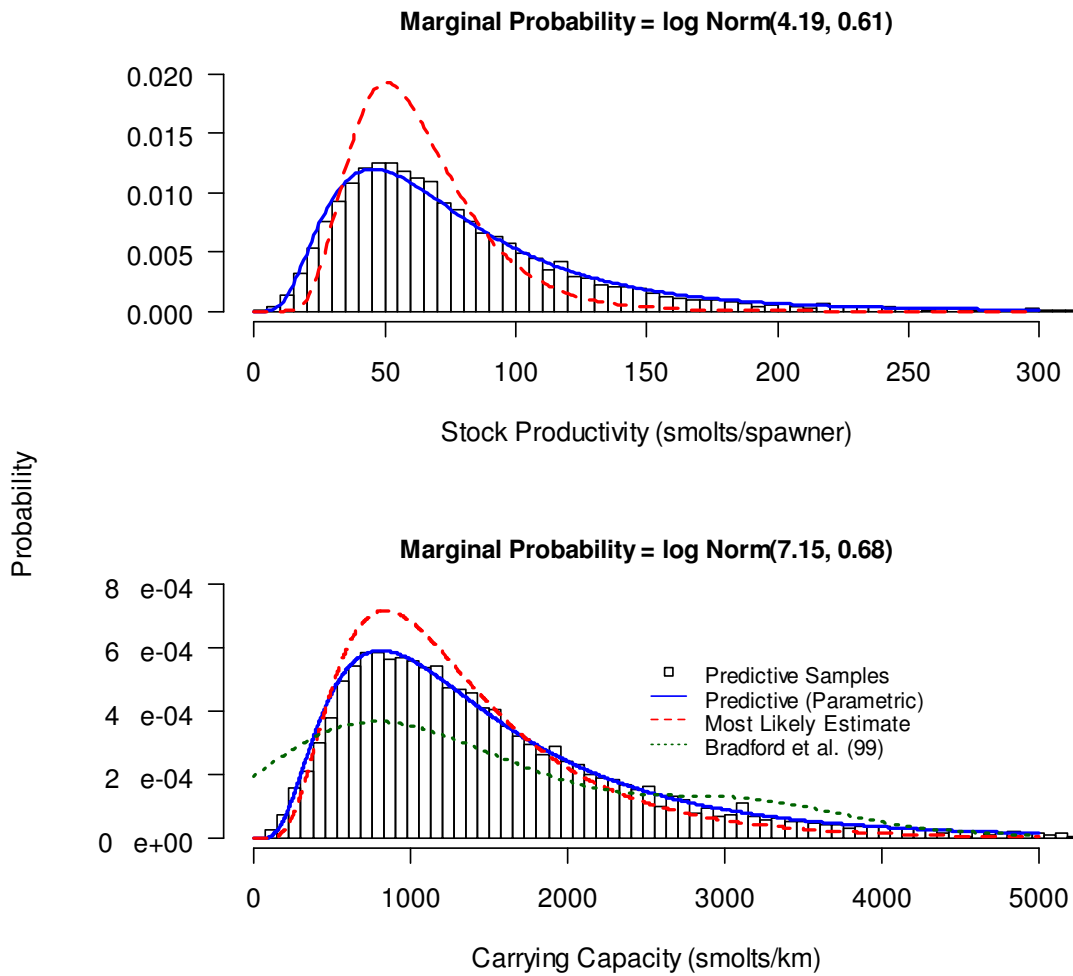


Figure 11. Marginal probabilities for the regional distributions of stock productivity and carrying capacity based on the hierarchical Logistic Hockey Stick model. The most likely estimates of the regional distributions are shown for reference.

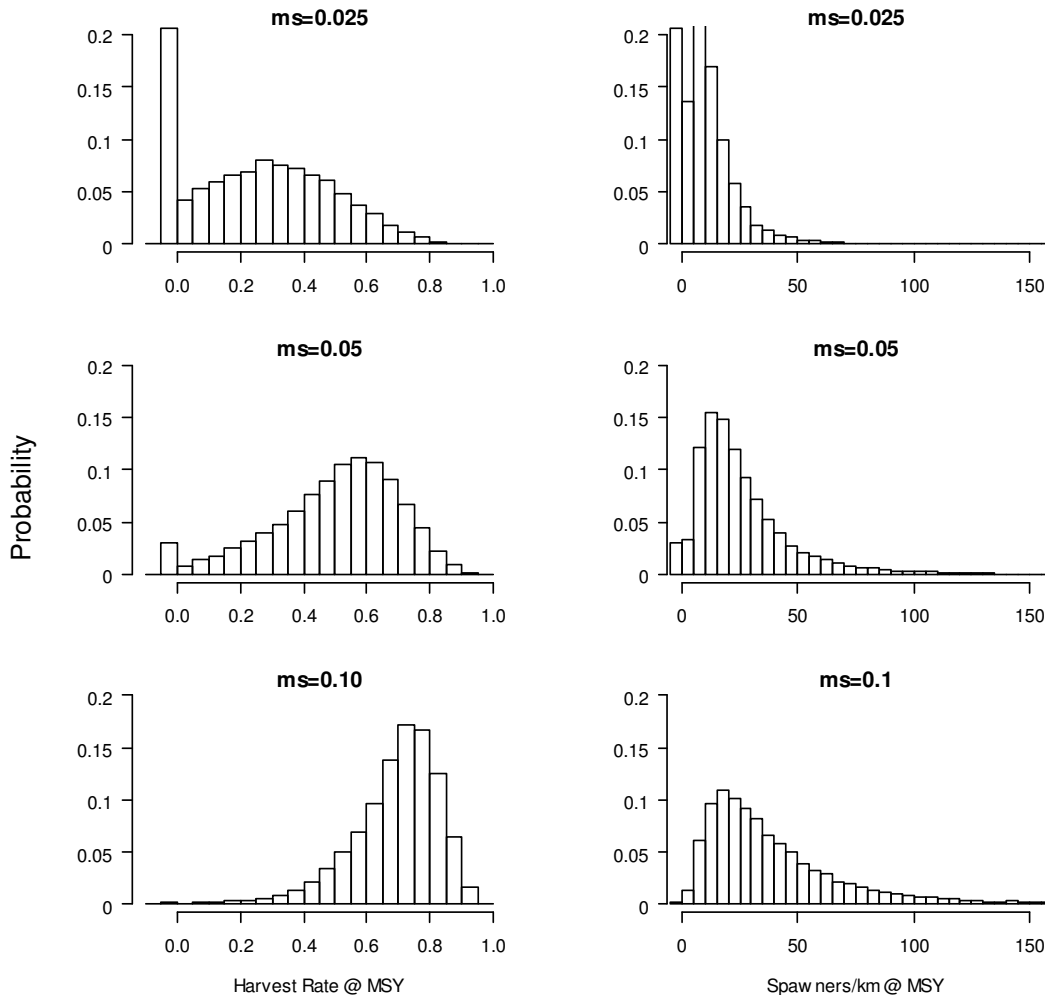


Figure 12. Marginal probabilities for harvest rates and escapements to produce maximum sustainable yield (MSY) at different marine survival rates (ms). Values <0 represent populations that are not sustainable even without harvest ($\alpha * ms < 1$). Results were computed from predictive marginal distributions of stock productivity and carrying capacity based on the hierarchical Logistic Hockey Stick model (Fig. 11).

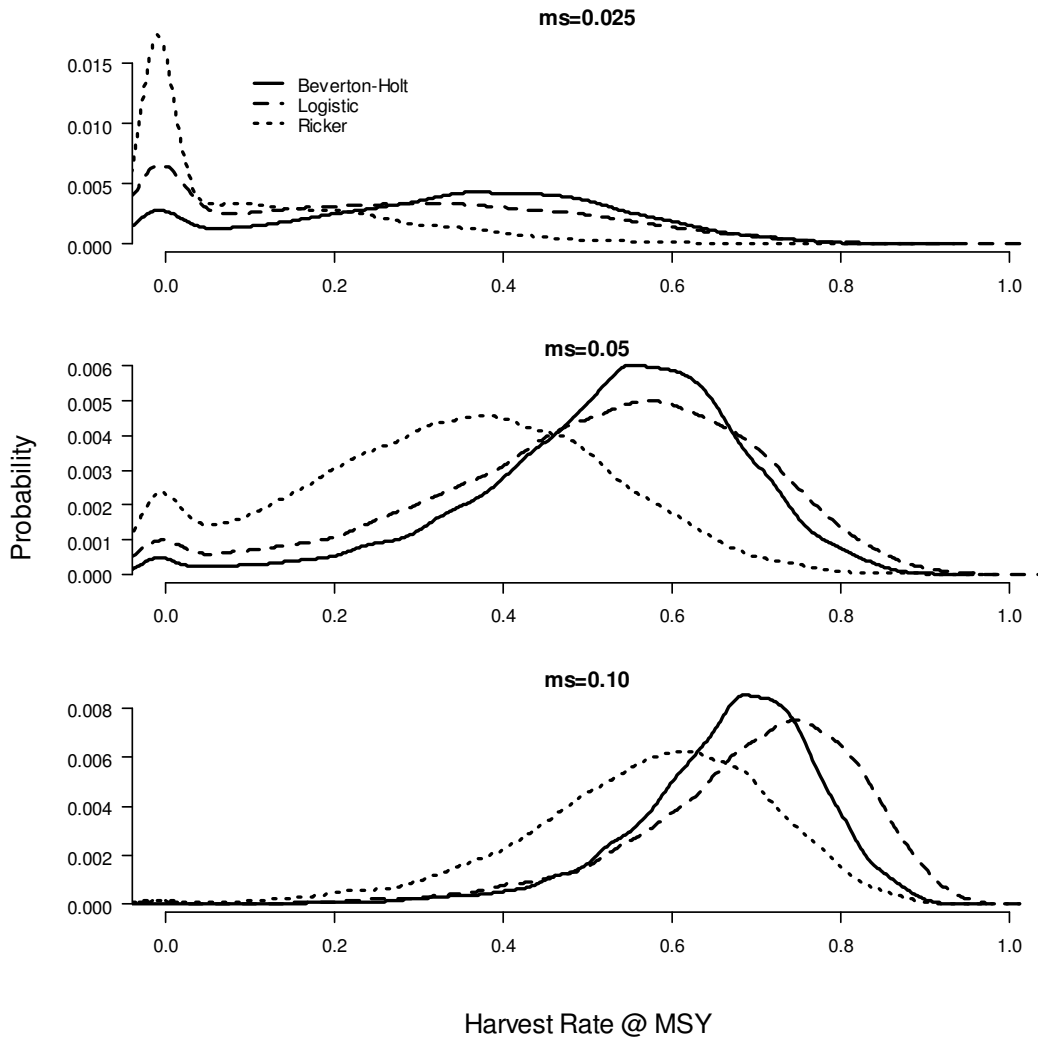


Figure 13. Comparison of marginal probabilities for harvest rates and escapements to produce maximum sustainable yield (MSY) for 3 stock-recruitment models at different marine survival rates (ms). Results were computed from predictive marginal distributions of stock productivity and carrying capacity.

a)

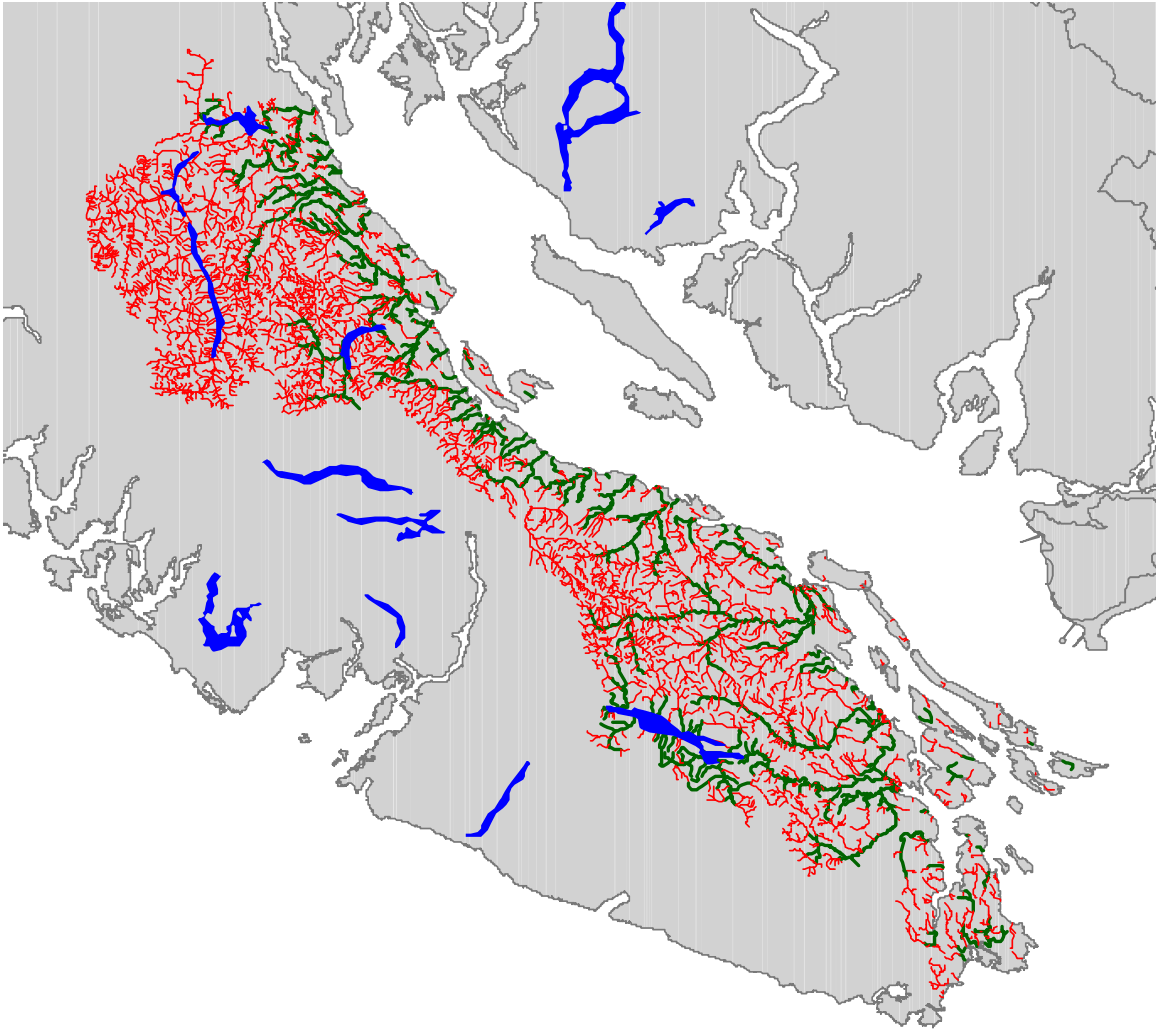


Figure 14. 1-50,000 Watershed Atlas showing the distribution of accessible (green) and inaccessible (red) coho habitat in the Georgia Basin West management unit (a) and the Thompson River drainage (b).

b)

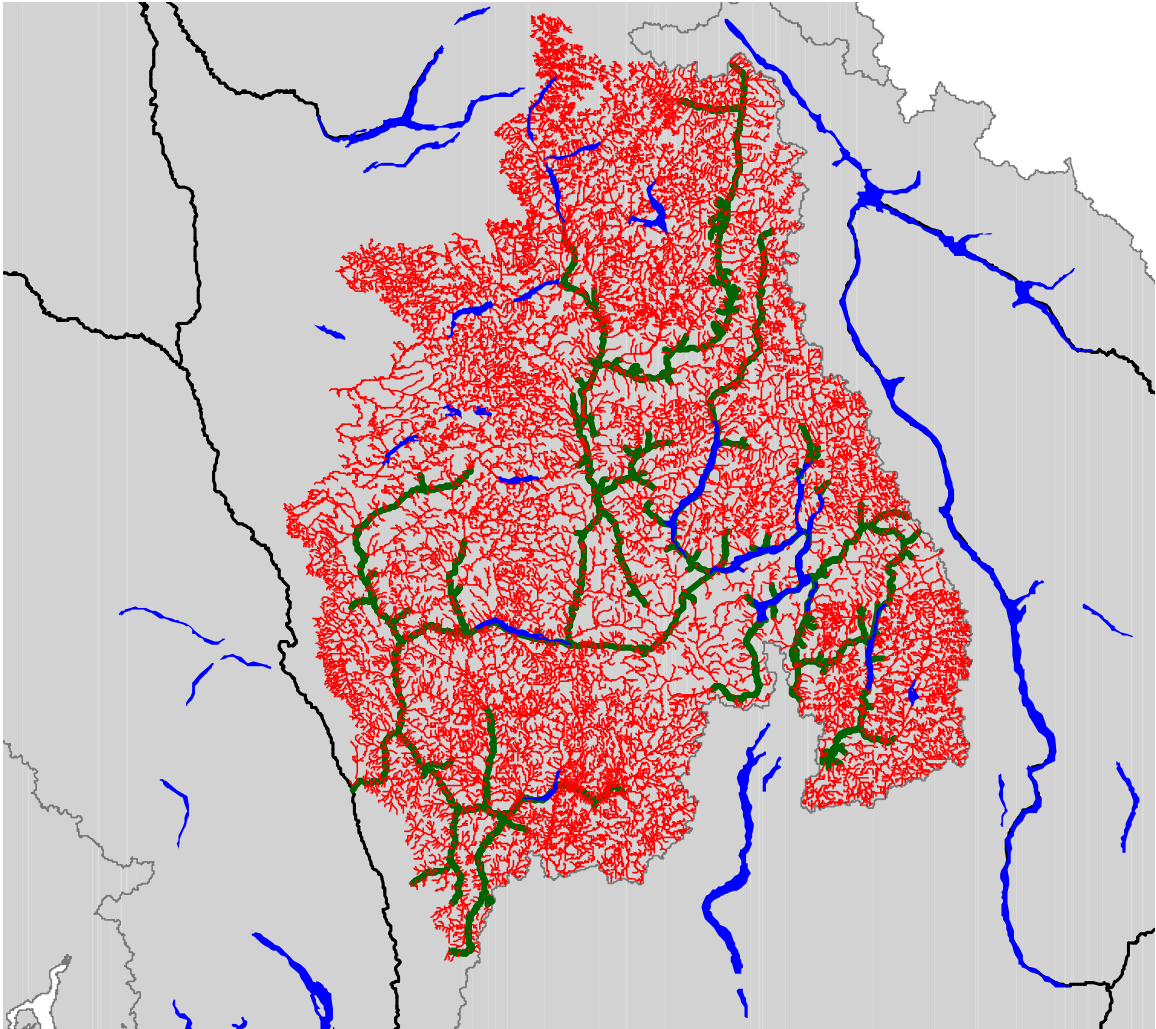


Figure 14. Con't.

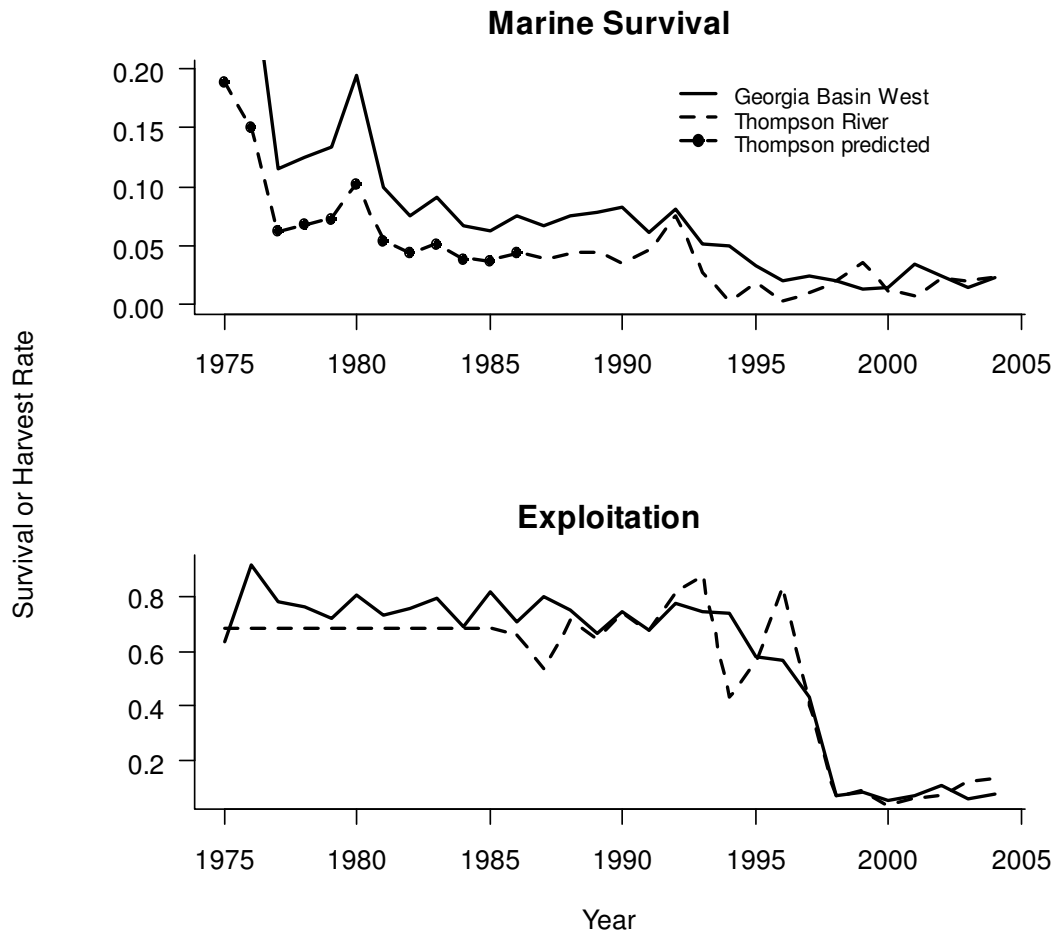


Figure 15. Aggregate marine survival and exploitation rates for populations in the Georgia Basin West management unit and the Thompson River drainage. Thompson survival rates prior to 1987 were predicted from the relationship between GBW and Thompson survival rates from 1987 to 2004.

a)

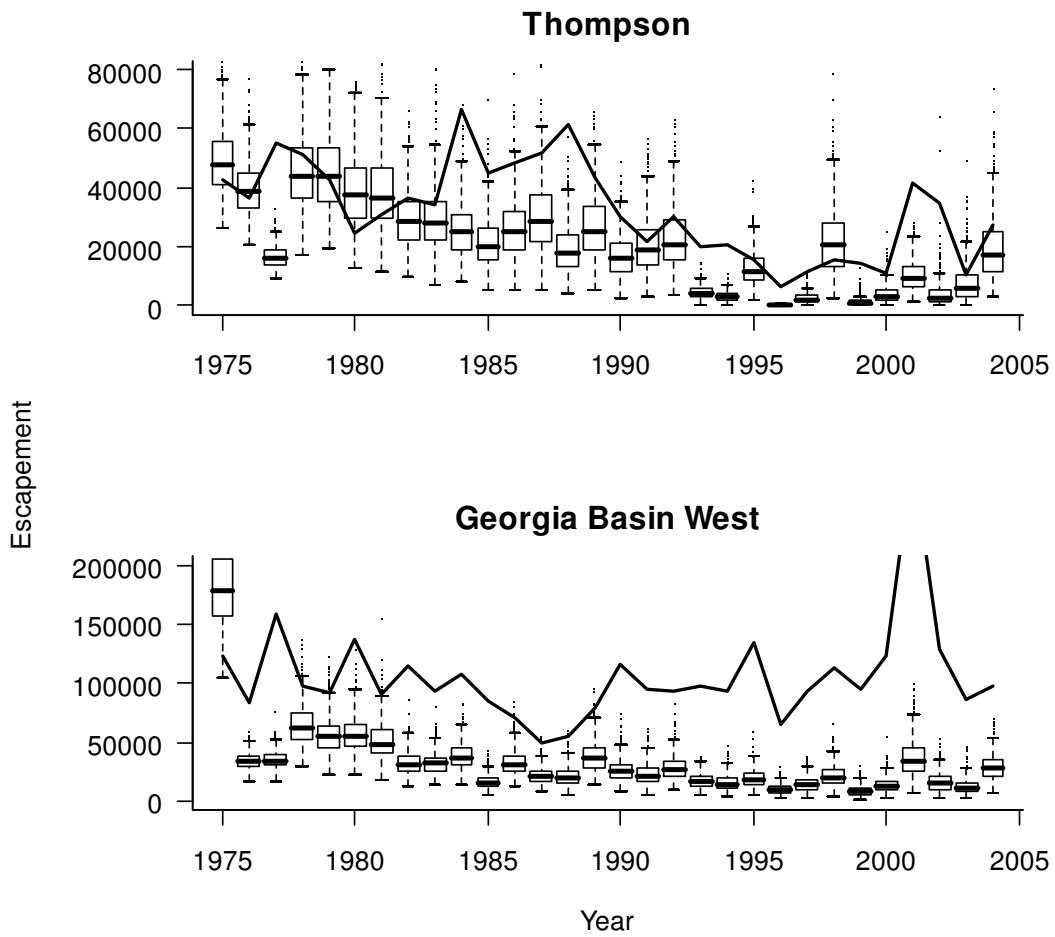


Figure 16. Simulated (box plots) and observed (lines) aggregate escapement trends in the Thompson River drainage and the Georgia Basin West management unit assuming 10 (a) and 90 (b) populations. Simulation results show the annual escapement distributions over 500 trails.

b)

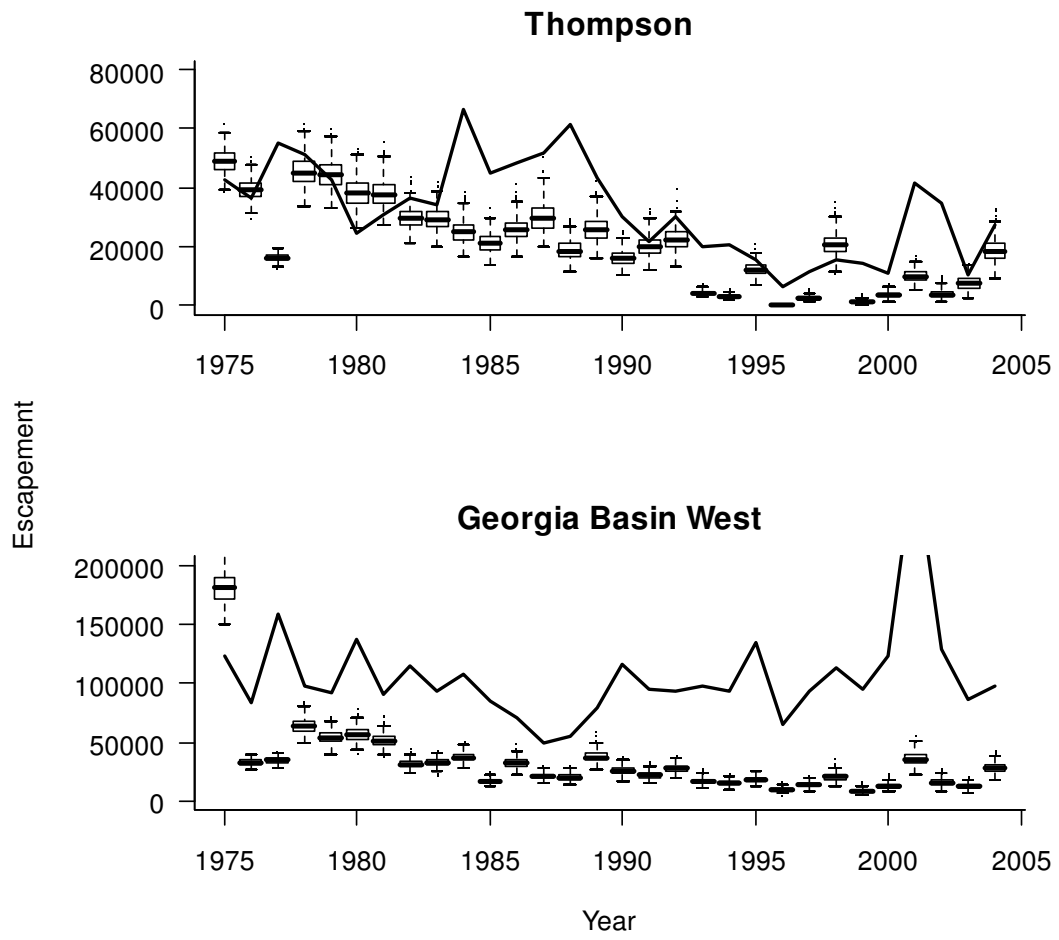


Figure 16. Con't.

Table 1. Sample size (n=years) for the 17 spawner-to-smolt datasets used in this analysis and the first and last year for each time series.

Population	n	First Yr	Last Yr
Big Beef	29	1976	2004
Big Qualicum	11	1961	1972
Bingham	10	1980	1989
Black	19	1985	2003
Carnation	32	1971	2002
Deschutes	17	1977	1996
Deer	13	1959	1971
Flynn	13	1959	1971
Hooknose	13	1947	1959
Hunts	11	1961	1971
Minter	11	1938	1953
Needle	12	1960	1971
Nile	5	1945	1951
Queets	20	1979	1998
Skagit	14	1989	2002
Skyhomish	11	1968	1984
Snow	18	1976	1996
Total	259		

Table 2. Values defining prior and hyper-prior distributions.

Parameter	Symbol	Distribution	Value
<i>Population-Specific Prior Parameters</i>			
Mean productivity	$\mu_{\alpha i}$	normal	80
CV for productivity	$CV_{\alpha i}$	normal	10
Carrying capacity	β_i	uniform	1-5000
Relative variance	σ_i	uniform	.001-20
<i>Hyper-Distribution Prior Parameters</i>			
Mean for μ_{α}	$\mu(\mu_{\alpha})$	normal	80
CV for μ_{α}	$CV(\mu_{\alpha})$	normal	10
Mean for μ_{β}	$\mu(\mu_{\beta})$	normal	1500
CV for μ_{β}	$CV(\mu_{\beta})$	normal	10
Mean for CV_{α}	$\mu(CV_{\alpha})$	inverse-gamma	1
Precision for CV_{α}	$\tau(CV_{\alpha})$	inverse-gamma	0.2
Mean for CV_{β}	$\mu(CV_{\beta})$	inverse-gamma	1
Precision for CV_{β}	$\tau(CV_{\beta})$	inverse-gamma	0.2

Table 3. Most likely spawner-to-smolt stock-recruitment parameter estimates for 3 hierarchical models. Stock productivity (α) and smolt carrying capacity (β) are in units of smolts/spawner and smolts/km, respectively.

	Beverton Holt			Logistic Hockey Stick			Ricker		
	α	β	σ	α	β	σ	α	β	σ
Hyper-Parameters (regional)									
Mean	86	1397		58	1154		43	1357	
CV	0.18	0.57		0.38	0.57		0.36	0.59	
Population-Specific Parameters									
Big Beef	79	1,882	0.29	40	1,623	0.29	35	1,839	0.30
Big Qualicum	88	3,012	0.47	104	2,319	0.39	30	3,396	0.62
Bingham	91	1,421	0.31	68	1,238	0.27	29	1,769	0.45
Black	84	2,519	0.49	53	2,127	0.50	43	2,676	0.52
Carnation	91	1,598	0.28	70	1,186	0.28	56	1,309	0.31
Deschutes	69	1,782	0.51	27	1,999	0.34	27	2,081	0.34
Deer	89	1,481	0.23	70	989	0.20	72	980	0.21
Flynn	85	612	0.60	58	487	0.63	41	659	0.68
Hooknose	94	1,034	0.29	77	853	0.26	58	971	0.28
Hunts	84	1,002	0.65	53	851	0.68	33	1,168	0.66
Minter	104	2,301	0.30	111	1,762	0.24	69	2,015	0.36
Needle	80	371	0.35	50	325	0.33	44	394	0.37
Nile	84	903	0.22	52	759	0.24	36	796	0.23
Queets	87	1,018	0.33	67	687	0.32	69	670	0.32
Skagit	85	1,977	0.33	50	1,620	0.34	34	1,909	0.34
Skyhomish	99	3,502	0.14	71	2,886	0.14	60	3,382	0.19
Snow	72	998	0.76	34	992	0.68	30	1,107	0.66
mean	86	1,613	0.39	62	1,336	0.36	45	1,595	0.40
median	85	1,481	0.33	58	1,186	0.32	41	1,309	0.34

Table 4. Standard deviation (SDR) and median absolute value (MAR) of Pearson residuals for most-likely fits of the hierarchical models to the spawner-to-smolt data.

Population	Beverton Holt		Logistic Hockey Stick		Ricker	
	SDR	MAR	SDR	MAR	SDR	MAR
Big Beef	1.02	0.64	1.02	0.76	1.02	0.8
Big Qualicum	1.04	0.96	1.22	0.77	1.05	0.78
Bingham	1.05	0.71	1.05	0.64	1.05	0.76
Black	1.03	0.74	1.03	0.64	1.03	0.74
Carnation	1.02	0.79	1.02	0.7	1.02	0.8
Deschutes	1.01	0.52	1.03	0.92	1.03	0.92
Deer	1.04	0.73	1.04	0.68	1.04	0.74
Flynn	1.03	0.81	1.03	0.65	1.03	0.63
Hooknose	1.04	0.58	1.04	0.74	1.04	0.86
Hunts	1.04	0.32	1.04	0.37	1.04	0.22
Minter	1.03	0.53	1.04	0.8	1.04	0.83
Needle	1.03	0.87	1.03	0.75	1.04	0.63
Nile	1.11	0.92	1.11	0.87	1.11	0.84
Queets	1.03	0.88	1.03	0.92	1.03	0.95
Skagit	1.04	0.54	1.04	0.76	1.04	0.46
Skyhomish	1.04	0.36	1.05	0.78	1.04	0.78
Snow	0.99	0.4	1.02	0.41	1.02	0.42
Mean	1.03	0.66	1.05	0.72	1.04	0.72

Table 5. Within-population correlations between estimates of stock productivity and carrying capacity based on Beverton Holt (BH), Logistic Hockey Stick (LHS), and Ricker (RI) hierarchical stock-recruitment models.

Population	Correlation Coefficient (r)			r ²		
	BH	LHS	RI	BH	LHS	RI
Big Beef	-0.71	-0.54	-0.12	0.50	0.29	0.01
Big Qualicum	-0.17	0.98	0.42	0.03	0.96	0.18
Bingham	-0.24	-0.04	0.56	0.06	0.00	0.31
Black	-0.47	-0.24	0.07	0.22	0.06	0.00
Carnation	-0.66	-0.35	-0.07	0.44	0.12	0.00
Dechutes	-0.68	-0.53	-0.53	0.46	0.28	0.28
Deer	-0.72	-0.47	-0.43	0.52	0.22	0.18
Flynn	-0.36	-0.37	-0.08	0.13	0.14	0.01
Hooknose	-0.4	-0.12	0.7	0.16	0.01	0.49
Hunts	-0.22	-0.44	0.4	0.05	0.19	0.16
Minter	-0.43	-0.11	0.43	0.18	0.01	0.18
Needle	-0.37	-0.11	0.64	0.14	0.01	0.41
Nile	-0.37	-0.25	0.04	0.14	0.06	0.00
Queets	-0.7	-0.54	-0.55	0.49	0.29	0.30
Skagit	-0.47	-0.54	-0.25	0.22	0.29	0.06
Skyhomish	-0.57	-0.29	0.46	0.32	0.08	0.21
Snow	0.4	-0.36	-0.18	0.16	0.13	0.03
mean	-0.42	-0.25	0.09	0.25	0.19	0.17

Table 6. Summary of small-sample Akaike (AIC_c) and Deviance (DIC) information criteria statistics for 3 hierarchical models.

a) AICc

Model	Log Likelihood	Deviance	# of Parameters	AICc	Δ AIC	AIC Weight
Beverton-Holt	-597.7	1195.4	55	1335.7	33.7	4.883E-08
Logistic Hockey	-580.9	1161.7	55	1302.0	0.0	1.000E+00
Ricker	-606.2	1212.5	55	1352.8	50.8	9.394E-12

b) DIC

Model	Average Deviance	Modal Deviance	# of Effective Parameters	DIC	Δ DIC	DIC Weight
Beverton-Holt*	1223.7	1187.6	36.1	1259.8	3.7	1.346E-01
Logistic Hockey	1220.8	1185.6	35.3	1256.1	0.0	9.571E-01
Ricker	1277.7	1235.2	42.6	1320.3	64.2	1.086E-14

* A weak prior on stock-specific productivity values ($\mu_{\alpha_i}=80$, $CV_{\alpha_i}=1$) was required to achieve convergence of the joint posterior distribution for the Beverton-Holt model.

Table 7. Number and length of streams that contain coho in the Georgia Basin West management unit and in the Thompson drainage by maximum stream order estimated from a summary of the BC Watershed Atlas. The number of streams with escapement records (SEDS) are also shown.

Maximum Stream Order	Georgia Basin West		Thompson River	
	# Streams	km	# Streams	km
1	73	93	9	5
2	87	218	20	28
3	62	404	26	72
4	15	295	34	236
5	6	291	21	764
6	2	34	5	597
7			3	566
Total	245	1,335	118	2,268
SEDS	97		87	

Table 8. Estimates of freshwater (smolts in millions of fish) and total (adult recruits) carrying capacity of the Georgia Basin West (GWB) management unit and the Thompson River drainage based on the mean smolt carrying capacity from the predictive marginal distribution (1642 smolts/km). Thompson capacities were computed using all accessible stream length and a subset of stream length that excluded large mainstems of 6th and 7th order. Adult recruitment is calculated as the product of smolt capacity and marine survival rates at 2.5%, 5.0%, and 10.0%. For reference, the average recruitment was calculated by expanding historical escapements by historical exploitation rates. The marine survival rates from index stocks over this period are also shown.

	Georgia Basin West	Thompson (all)	Thompson (≤5)
Habitat (km)	1335	2268	1105
Smolts (M)	2.19	3.72	1.81
Marine Survival (%)	Adult Recruits		
2.5%	55,000	93,000	45,000
5.0%	110,000	186,000	91,000
10.0%	219,000	372,000	181,000
Avg. Recruits (75-04)	334,000	95,000	
(75-04) Marine Survival	8.2%	4.7%	

Determining Canadian MU-Specific Reference Points

Part 2:

Comparison of the Fishery and Conservation Performance of Fixed- and Abundance-Based Exploitation Regimes for Coho Salmon in Southern British Columbia

Abstract

We compared alternate fixed- and abundance-based harvest rate policies for coho salmon in Southern British Columbia using a simulation model. The model consisted of a two-stage (spawner-smolt, smolt-adult recruit) population dynamics component and a management component that simulated error in recruitment forecasts and harvest implementation, and was parameterized based on an analysis of existing data. The model simulated the dynamics of multiple populations of differing productivity and capacity within a management unit. Performance under different harvest regimes was evaluated based on simulated yield, inter annual variability in yield, as well as conservation status of individual populations. We simulated fixed harvest rate policies ranging from 0.1 to 0.8 and abundance-based policies with a range of escapement floors, escapement ceilings, and harvest rates.

At the historical marine survival rate of 7%, catch was maximized at a fixed exploitation rate of 0.4. There was a near linear increase in the conservation failure rate as exploitation rates rose from 0.3 to 0.6. Rates greater than 0.4 resulted in a rapid increase in the fraction of stocks that were extirpated. Both yield and conservation statistics suggest there is little sense in harvesting coho at rates of greater than 0.4 unless marine survival increases beyond the historical average. The extent to which exploitation rate should be reduced to improve the status of weak stocks is hard to determine because the biological significance of reducing the conservation failure rate is highly uncertain. Abundance-based harvest regimes had much better performance than fixed exploitation rate regimes, but only in cases when they were compared to fixed exploitation rates that exceeded the rate where catch is maximized. Abundance-based harvest regimes performed poorly compared to fixed exploitation regimes when harvest rates at the escapement ceilings exceeded the optimal rate of 0.4. This occurred because the abundance-based harvest rate was determined from the recruitment of the aggregate stock. It was possible to overexploit weak populations and maintain an aggregate recruitment that was still large enough to justify relatively high harvest rates. There was little conservation or yield benefits associated with abundance-based policies compared to fixed exploitation strategies when the latter regime was based on a rate that optimized yield for the aggregate stock. Considering the increased costs of implementing

abundance-based strategies and the increased variability in yield, a fixed exploitation strategy is recommended. Reductions in harvest implementation error through better inseason management will likely lead to improvements in both conservation status of weak populations and fisheries yields.

Introduction

The objective of this analysis is to compare the efficacy of alternate fixed- and abundance-based harvest rate policies for coho salmon in Southern British Columbia. Walters and Parma's (1996) simulation analysis concluded that abundance-based harvest policies provided only marginally better yields compared to fixed harvest rate strategies, and produced much higher interannual variation in yield. They also showed that the performance of abundance-based strategies degraded much more rapidly compared to fixed harvest rate policies as the extent of management error increases. When they considered the much higher costs and challenges associated with accurately forecasting recruitment, they concluded that a fixed harvest rate policy is a better approach. This recommendation contrasts with the abundance-based policy that will be used to manage coho salmon in Southern BC if the fishery is reopened (Pacific Salmon Commission 2004). The rationale for the PSC policy is to allow some fishing but also promote rebuilding of coho stocks of conservation concern. Walters and Parma (1996) analysis was based on the recruitment dynamics of a single aggregate stock, and they did not consider the status of weak stocks that are part of the aggregate when assessing policies. In this analysis, we develop a model that simulates the dynamics of multiple populations within a DFO management unit (MU) with a range of productivities to compare fishery and conservation performance under different harvest policies.

The model consists of a population dynamics component that uses a Logistic Hockey Stick (LHS) spawner-to-smolt relationship that varies among populations within the MU. The number of returning pre-fishery recruits is predicted as the product of the smolt production and marine survival rate for each population, aggregated across all populations in the MU. Random variation in freshwater and marine survival rates is simulated, and includes the effects of temporal autocorrelation and across-stock correlations in deviations. A management component simulates an annual recruitment forecast that is used to determine exploitation rates for abundance-based harvest regimes, and also simulates implementation errors associated with realizing the target harvest rate. The model is used to evaluate harvest policies for populations in the Georgia Basin West management unit and the Thompson River drainage.

Methods

Model Structure

Population Dynamics

The population dynamic component of the model simulates the abundance of coho in both freshwater and marine portions of their life cycle. We assumed juveniles migrate to the ocean as age-1+ smolts only and spend 1.5 years in the ocean before returning to spawning areas to complete a 3-yr life cycle. The number of returning spawners for a single population i in yr t of the simulation is predicted from smolt abundance by assuming a constant or trending density-independent marine survival rate. The two-stage model is:

$$(1) \quad SM_{i,t} = f(SP_{i,t-2}) * e^{v_{i,t} - \frac{\sigma_f^2}{2}}$$

$$(2) \quad R_{i,t+1} = SM_{i,t} * MS_t * e^{v_{i,t} - \frac{\sigma_m^2}{2}}$$

$$(3) \quad SP_{i,t+1} = R_{i,t+1} * (1 - H_{i,t})$$

where, SM is the number of smolts/km of accessible stream length per population, SP is the number of returning spawners/km, R is the number of pre-fishery recruits/km, MS_t is the annual marine survival rate common to all stocks, and $H_{i,t}$ is the realized harvest rate on each population. $f()$ represents the Logistic Hockey Stick stock-recruitment function between spawners and smolts, and $v_{i,t}$ and $v_{i,t-2}$ are random deviates from normal distributions with a mean of 0 and standard deviations σ_f and σ_m ($N(0, \sigma)$). $\sigma^2/2$ is a lognormal bias correction term used so that the mean of random deviates is approximately 0. There is no straying among populations in a management unit as the number of smolts produced from each population depends only on the number of returning spawners for that same population. While straying and recolonization undoubtedly occurs within the meta-populations in each management unit, we assume that these processes have a relatively minor effect on population dynamics over the 25-generation simulation period.

The form of the Logistic Hockey Stick model (LHS, Barrowman and Myers 2000) is:

$$(4) \quad R_{i,t} = \alpha_i C \delta_i (1 + e^{\frac{-1}{C}}) \left[\frac{Sp_{i,t-2}}{C \delta_i} - \log\left(\frac{1 + e^{(Sp_{i,t-2} - \delta_i)/(C \delta_i)}}{1 + e^{\frac{-1}{C}}}\right) \right]$$

where,

$$(5) \quad \delta_i = \frac{\beta_i}{\alpha_i} \left[C(1 + e^{\frac{-1}{C}}) \left(\frac{1}{C} + \log(1 + e^{\frac{-1}{C}}) \right) \right]^{-1},$$

α_i is the initial slope of the stock-recruitment curve and is equivalent to the number of smolts produced per spawner at low density (stock productivity), and β_i is the maximum number of smolts that can be produced from the population per km of stream when stock size is not limiting (carrying capacity). C is a tuning parameter that determines the smoothness at the transition between the initial slope at low stock size and the asymptote at higher stock size. The logistic hockey stick model approaches the hockey stick model as $C \rightarrow 0$. In this simulation the tuning parameter was held constant at $C=1$.

Random deviations in freshwater and marine survival rates are assumed to be lognormally distributed (Bradford 1995). Deviations are autocorrelated across years and across populations based on the following algorithm. First, temporally autocorrelated annual deviates common to all populations for freshwater and marines survival are computed from:

$$(6) \quad v_t = v_{t-1} * \rho_{y,f} + N(0, \sigma_v) * \sqrt{(1 - \rho_{y,f}^2)}$$

$$(7) \quad v_t = v_{t-1} * \rho_{y,m} + N(0, \sigma_v) * \sqrt{(1 - \rho_{y,m}^2)}$$

where $\rho_{y,f}$ and $\rho_{y,m}$ are the lag-1 autocorrelation coefficients in deviates from the spawner-to-smolt relationship and deviates from the average marine survival rate, respectively. Note that when $\rho_y = 0$ there is no autocorrelation in survival rates. Population-specific deviates are then computed from the annual common deviates and the extent of inter-correlation among stocks from:

$$(8) \quad v_{i,t} = v_t * \rho_{p,f} + N(0, \sigma_f) * \sqrt{(1 - \rho_{p,f}^2)}$$

$$(9) \quad v_{i,t} = v_t * \rho_{s,m} + N(0, \sigma_m) * \sqrt{(1 - \rho_{s,m}^2)}$$

where, $\rho_{p,f}$ and $\rho_{p,m}$ are the inter-stock correlation coefficients based on the deviations from the spawner-to-smolt relationship and the average marine survival rate, respectively.

The total pre-fishery recruitment to the management unit (R_t) is simply the product of the stream length-standardized recruitment and the length of stream for each population (km_i), summed across all populations ($Npops$),

$$(10) \quad R_t = \sum_{i=1}^{Npops} R_{i,t} * km_i$$

The length of stream for each population is simply the total stream length for the simulated area (e.g. Georgia Basin West or the Thompson River drainage) divided by the number of populations that are simulated.

Management Dynamics

The forecast of the total number of recruits is the product of the actual recruits and deviates that depend on the magnitude of forecast error,

$$(11) \quad \hat{R} = R_t * e^{\kappa_t - \frac{\sigma_\kappa^2}{2}}$$

where κ_t is a random deviate from a normal distribution with a mean of 0 and a standard deviation σ_κ . The target harvest rate each year (TH_t) is determined from:

$$(12) \quad \begin{aligned} TH_t &= H_{\min} \mid \hat{R}_t < E_{\min} \\ TH_t &= H_{\max} \mid \hat{R}_t > E_{\max} \\ TH_t &= H_{\min} + (\hat{R}_t - E_{\min}) \left[\frac{H_{\max} - H_{\min}}{E_{\max} - E_{\min}} \right] \mid E_{\min} \leq \hat{R}_t \leq E_{\max} \end{aligned}$$

where, H_{\min} and H_{\max} are the minimum and maximum exploitation rates and E_{\min} (escapement floor) and E_{\max} (escapement ceiling) are the aggregate escapement for the MU when those rates apply, respectively. Harvest rates at intermediate escapements are determined by linear interpolation. Setting $E_{\min}=0$ eliminates the escapement floor, that is fishing continues regardless of how low the forecasted recruitment is. A fixed harvest rate policy is simulated by setting $E_{\min}=E_{\max}=0$ and setting $H_{\min}=H_{\max}$ to H , the desired fixed exploitation rate. For fixed harvest rate policies, we assumed the desired rate will be achieved through time-area closures and that recruitment forecasts are not needed to achieve the target rate. This contrasts with the abundance-based rule, where recruitment forecasts are required to determine what harvest rate to use. Note that eqn. 12 is simply a continuous version of the 3-level abundance based harvest rate rule proposed by PSC

(2004). Eqn. 12 results in harvest rate scaling proportionally with abundance in between E_{\min} and E_{\max} , while the PSC-type approach results in stepped change in harvest rate.

The average harvest rate applied across stocks (H_t) is a product of the target harvest rate and a deviate that accounts for the error in attaining an average harvest rate,

$$(13) \quad H_t = TH_t * e^{\lambda_t \frac{\sigma_\lambda}{2}}$$

where λ_t is a random deviate from a normal distribution with a mean of 0 and a standard deviation σ_λ . This error reflects the difficulty in achieving the desired mean harvest rate that would result from changes in the spatial and temporal distribution of the aggregate run as it passes through fishing areas. Population-specific harvest rates are calculated as the product of the mean harvest rate and a deviate that accounts for the variation in harvest rates among populations due to population-specific differences in run timing and holding patterns in relation to the time and area closures of the fishery,

$$(14) \quad H_{i,t} = H_t * e^{\eta_t \frac{\sigma_\eta}{2}}$$

where η_t is a random deviate from a normal distribution with a mean of 0 and a standard deviation σ_η . $H_{i,t}$ is substituted into eqn. 3 to determine the spawning escapement for each population. The total catch in each year for the management unit ($Total_Catch_t$) is simply the sum of catches across all populations,

$$(15) \quad Total_Catch_t = \sum_{i=1}^{Npops} R_{i,t} * H_{i,t}$$

The performance of each harvest rate policy is evaluated based on five metrics that characterize the fishery in terms of average yield, interannual variation in yield, and the conservation status of the populations within the management unit. The metrics are:

1. the total catch from the MU, averaged across all years of the simulation;
2. the coefficient of variation (CV) in total catch across years;
3. the total escapement to the MU, averaged across years;
4. the percentage of years where the population-specific spawning escapements are below a pre-determined conservation limit, averaged across all populations; and
5. the percentage of populations that are extirpated. Extirpation is assumed to occur when the number of spawners is less than 2 fish in the last 3 consecutive years of the simulation.

The conservation failure metric aggregates performance across populations and is a compact measure of summarizing conservation status. Its limitation is that the same failure rate could result from few populations being below the conservation limit a high proportion of the time, or many populations dropping below the limit on only rare occasions. We therefore also kept track of the percentage of populations by conservation failure category (i.e., 0-10% failure, 10-20%, ...90-100%). The conservation metric is also dependent on a somewhat arbitrary limit. We therefore categorized the population-specific escapements by computing the percentage of years by escapement class (0-3 spawners/km, 3-6, 6-9, ... ,57-60/km). Performance statistics were averaged over the total number of trials simulated for each harvest policy.

Model Parameterization

Model parameters for population dynamics were determined from analysis of data from index populations. The Logistic Hockey Stick stock-recruitment model was used in this analysis over Beverton-Holt and Ricker models because it had the best out-of-sample predictive power, and avoided biases in stock productivity and density dependent compensation apparent in the other models (Korman and Tompkins 2007). On each simulation trial, stock productivity and carrying capacity parameters for each population are randomly selected from the marginal predictive posterior distributions of parameters developed from a hierarchical meta-analysis using data from 17 populations (Korman and Tompkins 2007). We used the median standard deviation of the 17 most likely spawner-to-smolt relationships estimated in the hierarchical analysis (see Table 3 of Korman and Tompkins 2007) to simulate the extent of variation in freshwater survival rate (Table 1). The lag-1 autocorrelation in deviates from the spawner-to-smolt relationship was estimated using the average lag-1 autocorrelation in the standardized Pearson residuals from the most likely stock-recruitment curves for each of the 17 populations (Fig. 4 of Korman and Tompkins 2007). The interpopulation correlation was also estimated from the same standardized residuals. We used simulation to determine the appropriate value of $\rho_{p,f}$ applied to set of 1000 common deviations to generate the extent of inter-population correlation seen in the data.

The mean marine survival rate used in the simulations was the arithmetic average of 8 DFO index stocks (Big Qualicum, Chilliwack, Inch, Quinsam, Robertson, Carnation,

Black, Salmon) of 0.07 (Table 1). All marine survival time series ranged from brood years 1986-2004 with time series for 3 index stocks extending back to 1975. We also simulated a marine survival rate of 0.035 under the assumption that the historical average is twice the survival rate of the expected future conditions. The interannual standard deviation (SD) in marine survival was determined from the log-transformed values of these same data (Table 1). The lag-1 autocorrelation coefficient and interstock correlation in marine survival was computed from these same data using the same methods described for the analogous freshwater components.

There was very limited data to parameterize the management component of the model. Time series models are currently used to forecast marine survival for coho populations in Southern British Columbia. These models explain between 50 and 60% of the variation in marine survival for Black Creek and the Salmon River (Simpson et al. 2004). A simulated value of $\sigma_{\kappa}=0.5$ is required to generate the same correlation (Table 1). However, this should be considered a conservative estimate of uncertainty in recruitment forecasts because adult recruitment will also depend on aggregate smolt production, which is only measured at a few index streams within each management unit. Current recruitment forecasts do not consider escapement or smolt production data. Thus we also simulated a higher level of recruitment forecast error of 0.75. There were no data available to estimate the extent of error in attaining the target harvest rate averaged over all stocks, and the extent of variation in harvest rates applied to individual stocks. We simulated arbitrary σ_{λ} and σ_{η} values of 0, 0.25, and 0.5.

The total length of accessible rearing habitat (Tkm), used to determine the length of productive habitat for each population ($km_i = Tkm/Npops$) was estimated from the 1-50,000 digital Watershed Atlas (WA). Korman and Tompkins (2007) determined there are 1,335 and 2,268 km of accessible habitat for the Georgia Basin West management unit and the Thompson River drainage, respectively (see Table 7 and Fig. 14 and 15 of Korman and Tompkins 2007). Based on a comparison of observed adult recruitment and estimates derived from the product of Tkm, average smolt capacity per km of stream, and a range of historical marine survival rates, they concluded that the GBW habitat estimate was reasonable, but that the Thompson estimate produced too many smolts (see Table 8 of Korman and Tompkins 2007). By eliminating large mainstem reaches from the habitat

calculations, accessible stream length for the Thompson was reduced to 1105 km. This value produced an adult recruitment that was reasonably close to historical estimates and was therefore used in this analysis.

There were not sufficient data to use different parameter estimates for GBW and Thompson simulations. There were no spawner-to-smolt data from interior streams used in the analysis of Korman and Tompkins (2007). This analysis must therefore assume that the marginal predictive distributions of freshwater stock-recruitment parameters apply in both GBW and the Thompson. The distributions appear to be relatively conservative for both areas, predicting a more rapid decline in spawner abundance under historic marine survival and harvest regimes than was evident in the SEDS escapement data (see Fig. 16 of Korman and Tompkins 2007). Marine survival trends from GBW and Thompson index stocks were similar over the available time series and of similar scale in the last decade, and historical exploitation rates have also been very similar (see Fig. 15 of Korman and Tompkins 2007). Given the similarities and data limitations, there is no justification to use different parameter estimates for GBW and Thompson simulations. The only difference in regions that was apparent in the data was the amount of accessible stream length, however this difference was only 230 km. Considering the large uncertainty in the true amount of rearing habitat that limits coho production in these large areas, we used an average value of 1200 km for both systems. This allowed us to use the same set of simulations for both GBW and the Thompson, greatly reducing the volume of results.

We assumed that both the GBW MU and the Thompson River drainage consist of 100 independent coho populations. The analysis of data in the Watershed Atlas determined that there were over 200 and 100 unique streams that contained coho in GBW and the Thompson, respectively (see Table 7 of Korman and Tompkins 2007). Excluding 1st and 2nd order streams in both systems, and 6th and 7th order reaches from the Thompson, resulted in 85 and 81 streams containing coho in GBW and the Thompson drainage, respectively. There are approximately 90 unique streams in each area that have a long-term escapement record for coho. Thus, modeling 100 independent populations is roughly equivalent to the spatial detail of escapement estimates and the number of moderate size streams (3rd-5th order) that are accessible to coho. Given 1200 km of total stream length, the length of stream for each population (km_i) is 12 km.

It is important to note that the actual number of populations that are simulated will not influence any of the model results except perhaps the extirpation statistic. All calculations are carried-out per unit of accessible stream length. For example, spawner density (fish/km) is compared to the length-standardized conservation limit (6 spawners/km) so the number of populations will not influence the conservation failure metric. Total recruitment to the management unit is simply the product of length-standardized recruitment and the total productive stream length for each population. If the number of populations is reduced, the stream length for each population will increase leading to the same aggregate recruitment predictions, and hence the same catch. Simulating fewer populations will result in more inter-trial variance (e.g. Fig. 16 of Korman and Tompkins 2007), however we would compensate for this by increasing the number of trials to maintain the same precision on across-trial average performance metrics. The percentage of stocks that are extirpated is the only metric that may depend on the number of populations that are simulated because the annual absolute escapement for each population is compared to a value of 2, the minimum number of fish required for reproduction. Increasing the number of populations reduces absolute population size and therefore could increase the number of populations that decline below 2 fish. However, since the statistic is expressed as the percentage of populations that fail to meet the criteria, the percentage may not change with an increase in the number of populations that are simulated.

We simulated fixed harvest rate policies ranging from 0.1 to 0.8 in 0.1 increments. Abundance-based policies were simulated using a range of escapement floors, escapement ceilings, and harvest rates. The escapement floor at which the minimum harvest rate is used (Esc_{min}) was set 7,200 or 25,000 spawners. The former limit is equivalent to the number of spawners required to meet the absolute conservation limit for the aggregate population ($7,200 = 6 \text{ spawners/km} * 1200 \text{ km of accessible stream length}$). The latter value is equivalent to the conservation reference point of Irvine et al. (2001) based on 25% of the historical peak spawner abundance and is equivalent to a spawner density of 20 fish/km. The escapement ceiling at which the maximum harvest rate is used (Esc_{max}) was set at 25% (33,600), 50% (67,200), and 75% (100,800) of carrying capacity at default conditions. Adult carrying capacity was estimated at 134,400 based on the

product of the mean smolt capacity per km of stream from the marginal predictive distribution of Korman and Thompkins (1600 smolts/km), total habitat length (1200 km), and the average historical marine survival rate (0.07). The harvest rate at the escapement floor (H_{\min}) was set at 0.1 based on the assumption that some coho will be harvested incidentally as bycatch in sport and commercial fisheries even when the southern BC commercial coho fishery is closed. The harvest rate at the escapement ceiling (H_{\max}) was set at values of 0.4, 0.6, and 0.8

A total of 75 years was simulated for each trial. Each population was seeded with 1,344 spawners or 112 spawners/km, the number required to meet carrying capacity (134,400/100 populations). We also initialized the population at 25% of this value. The first 15 years of the simulation are treated as initialization years and predictions in this time period are not used when computing performance statistics. Thus, the simulation results are based on the last 60 years or 20 coho generations. 1000 trials were simulated for each harvest policy, which was sufficient to reduce the CV in the cumulative average performance statistics to < 1%.

Results

A comparison of performance measures across fixed harvest policies ranging from 0.1-0.8 demonstrates the correlation among conservation statistics, and the trade-off between fishery and conservation performance (Fig. 1). Under a fixed exploitation strategy, the aggregate escapement to the MU decreases as harvest rate increases and conservation failure rate and the proportion of populations that are extirpated increase. Conservation metrics were strongly correlated with each other: escapement explained 93% and 74% of the variation in conservation failure and extirpation rates, respectively, and the conservation failure rate explained 91% of the variation in the extirpation rate. The average catch reached a maximum value of approximately 40,000 fish at a harvest rate of 0.4. The interannual CV in catch was relatively stable up to harvest rates of 0.5, after which it increased exponentially as a result of overexploitation. Harvest rates greater than 0.5 at an expected marine survival rate of 0.07 did not perform well in terms of both fishery or conservation performance. At harvest rates up to 0.4 there was a near linear tradeoff between yield and conservation.

The distribution of spawner density and conservation failure rates across populations is shown for a fixed harvest rate of 0.4 (Fig. 2) to better understand conservation measure statistics. The conservation failure rate at this harvest rate was 35%. 54% of the populations fell below 6 spawners/km less than 20% of the simulated years, 42% had a failure rate between 20 and 60%, and the remaining 8% had a failure rate of 90-100% (Fig. 2, top). The distribution of spawner densities across populations and years is useful for understanding the limitations of the conservation failure rate statistic. In this example, the failure rate is 35%, but there is also a large fraction of cases with relatively low spawner abundance not accounted for in the metric (e.g. 23% with densities between 6 and 21 spawners/km).

Model performance was very sensitive to the assumed marine survival rate. We reran the fixed harvest rate policy under a marine survival rate of 0.035, $\frac{1}{2}$ the historical average. At lower survival, the exploitation rate at which catch was maximized declined and occurred over a broader range of 0.2-0.4. At lower survival, catches were reduced by 3- to 5-fold, and conservation failure rates were 2- to 3-fold higher (Fig. 3).

Fixed and abundance-based harvest regimes are compared in Table 2. The abundance-based policy with $H_{\max}=0.8$ performed poorly relative to the fixed harvest regime. The realized exploitation rates decreased as the escapement floor and ceilings were raised, but the effective rates were still high and ranged from 51-63%. Thus, in spite of limiting harvest rates to levels substantially below the maximum rate of 0.8, the regime was fundamentally too aggressive. As a result, CV in catch was much higher as were the conservation failure and extirpation rates. The abundance-based regime depends on the recruitment of the aggregate stock and can therefore be insensitive to the abundance of weak populations.

The abundance-based regime at $H_{\max} = 0.4$ had considerably better performance than the equivalent $H_{\max}=0.8$ regime (Table 2). There was little difference in yield and conservation statistics across the escapement floors and ceilings that were used. The realized harvest rate under these conditions had a very limited range (34-39%) indicating that the forecasted recruitment was on average close to the ceiling. The abundance-based regime at $H_{\max}=0.6$ had only slightly better yield than the $H_{\max}=0.4$ policies but considerably higher conservation failure rates and modestly higher variation in catch.

There was much more sensitivity to escapement floors and ceilings under the $H_{\max}=0.6$ and 0.8 regimes. As H_{\max} is reduced, abundance-based policies converge to a fixed exploitation strategy and therefore become less sensitive to the escapement floor and ceilings that are used to define them.

Abundance-based harvest regimes outperformed constant harvest rate regimes, but only in cases when the fixed harvest rates were well beyond the rates that were sustainable for the majority of populations in the MU (Table 2). The $H_{\max}=0.6$ and 0.8 abundance-based regimes had much better performance than fixed policies at $H=0.6$ and 0.8, respectively. The best abundance-based regime at $H_{\max}=0.4$ had slightly better performance compared to the fixed harvest regime at $H=0.4$. To ensure that this difference was not due to interpolation errors, we reran the fixed harvest rate regime in increments of 0.01. Maximum yield of 39,220 occurred at an exploitation rate of 0.42 with a corresponding conservation failure rate and CV of 37% and 76%, respectively. Yield and conservation statistics were still marginally better under the abundance-based $H_{\max}=0.4$ regime.

The effects of management error on model performance varied by harvest rate regime and error type. The fixed harvest rate policy was not affected by increases in the extent of forecast error (Table 3) as recruitment forecasts were not used to determine exploitation rates. Higher forecast error resulted in only a minor decrease in yield statistics and very small changes in conservation statistics for abundance-based rules. We ran additional simulations with high and low forecast error in the absence of any implementation error and still observed little sensitivity to forecast error. In contrast, higher rates of harvest implementation error substantially degraded conservation and yield statistics under both fixed- and abundance-based harvest regimes. Increasing implementation errors from $\sigma_{\lambda} = 0.25$ to 0.5 reduced yield and conservation performance by 30-40%. Decreasing implementation error had much less of an effect ($\sigma_{\lambda} = 0.25$ to 0) than the equivalent increase. Performance statistics were equally sensitive to changes in error in the average harvest rate (σ_{λ}) or the population specific rates (σ_{η}).

We repeated the fixed harvest rate and abundance-based exploitation regimes ($H=H_{\max}=0.4$) using an initial stock size that was 25% of carrying capacity which is likely more indicative of current conditions, at least for the Thompson River drainage

averaged over the last 5 years. Performance statistics were indistinguishable from those presented in Table 2. This occurred because the initialization period was 15 years long or 5 generations, sufficient time for the population to achieve equilibrium conditions under the current harvest regime before the 60-year period over which statistics were computed.

Discussion

We compared the conservation and fishery performance of a range of fixed- and abundance-based harvest regimes using a simulation model. Although there is a considerable history of such exercises (see Hilborn and Walters 1992), our effort was relatively unique because it considered the variation in productivity in populations within a management unit that experience a common exploitation regime. We also tracked the performance of both fishery and conservation statistics, and parameterized the model based on an extensive analysis of existing data. The modelling suggests that a maximum sustainable yield for coho salmon in Southern BC will be obtained at a fixed harvest rate of 0.4 assuming conditions summarized in Table 1. This exploitation rate is roughly half of the rate that populations in southern BC were exposed to historically. Korman and Tompkins (2007) used a hierarchical meta-analysis to estimate stock productivity and harvest rates at MSY (U_{msy}). Their analysis suggested $U_{msy}=0.6$ for a population with average productivity at a marine survival rate of 0.07 (calculated from the same analysis used to generate Fig. 12 of Korman and Tompkins 2007). The U_{msy} value of 0.4 reported here is considerably lower in part because the simulation model includes the effects of harvest implementation error, while static analyses such as Korman and Tompkins (2007) and Chen and Holtby (2002) do not. U_{msy} increased from by 25% to 0.5 when we eliminated all management error in the simulations. This value was still lower than the estimate of 0.6 from Korman and Tompkins (2007) because the U_{msy} for a population of average productivity within the aggregate is not equivalent to the harvest rate that maximizes the yield for the entire aggregate stock. The difference occurs because the U_{msy} distribution for populations in the aggregate is skewed towards lower values, and because there is a cost to future yields due to overexploitation, but no future consequence of underexploitation.

The simulation exercise demonstrated that while a fixed exploitation rate of 0.4 produces the maximum sustainable yield, lower harvest rates improve the conservation status of weak stocks. There was a near linear increase in the conservation failure rate as exploitation rates rose from 0.3 to 0.6. Rates greater than 0.4 resulted in a rapid increase in the fraction of stocks that were extirpated. Both yield and conservation statistics suggest there is not much sense in harvesting coho at rates of greater than 0.4 given model assumptions. The extent to which this value should be reduced to improve the status of weak stocks is hard to determine because the biological significance of reducing the conservation failure rate is unknown. Extirpation rates at harvest rates of 0.4 or less were very low but our model does not include any compensatory mortality processes and may therefore underestimate the risk of sustained low population size. Catch and conservation performance degraded substantially when the assumed marine survival rate was reduced from 0.07 to 0.035. Catch was low and conservation failure was relatively high even at very low exploitation rates.

Abundance-based harvest regimes performed poorly compared to fixed exploitation regimes when harvest rates at the escapement ceilings exceeded the U_{msy} rate of 0.4. This occurred because the abundance-based harvest rate is determined from the recruitment of the aggregate stock. Thus, it is still possible to overexploit weak populations and maintain an aggregate recruitment that is large enough to justify relatively high harvest rates. Abundance-based harvest policies will only be effective at protecting weak populations if they are determined based on the recruitment forecasts for the weak populations. We did not simulate this scenario because it is well beyond current DFO forecasting practices which are based exclusively on prediction of marine survival rates and do not include spawning escapement or smolt production from index streams as covariates.

The analysis demonstrated that abundance-based harvest regimes are considerably better than fixed exploitation rate regimes if the fixed exploitation rate is too high. However, abundance-based regimes had considerably reduced performance relative to a fixed regime using an exploitation rate equivalent to U_{msy} , determined from the aggregate response of multiple populations ($U_{msy} = 0.4$). Abundance-based harvest regimes had equivalent or marginally better performance relative to fixed harvest rate regimes when

the harvest rate at the escapement ceiling was equivalent to U_{msy} . Realized exploitation rates under such policies were quite close to the maximum rates that occur at the escapement ceiling, thus there was little difference between abundance- and fixed-rate regimes in this case. Considering the small improvements in yield and conservation and the increased interannual variation in catch, this analysis provides little support for an abundance-based harvest rate regime defined by the aggregate recruitment.

This analysis suggests that reductions in harvest implementation error through better inseason management might lead to improvements in both conservation status of weak populations and fisheries yields. Under the fixed harvest regime, reducing harvest implementation error relative to the baseline had little effect, but increasing it resulted in a large decrease in fishery and conservation performance. The sensitivity to management error depended on the relative variance of management and process errors as well as other aspects of population dynamics. When implementation error was eliminated, conservation and fishery performance was determined by population dynamic characteristics. There is a limit to how much yield and conservation statistics can be improved given the assumed extent of natural variation and the fact that a common harvest rate is being applied to populations with a range of productivities. When implementation error is high enough, its effects begin to dominate the effects of population dynamics, and performance is degraded. Unfortunately, because the simulated implementation errors used here were arbitrarily defined, it is uncertain where the simulated values lie relative to the real extent of management error in a future fishery. If the actual error rate is equivalent to the maximum value we have simulated, reductions in implementation error due to better inseason management will improve fishery performance and conservation status. Accurate estimation of population-specific exploitation rates in future fisheries would help define the error rate and resolve this uncertainty.

Performance measures were not sensitive to forecast error. This was expected for the fixed exploitation rate policies that do not depend on recruitment forecasts, but was surprising for abundance-based regimes that do. This result was obtained for a range of scenarios not shown here that included reduced forecast error with and without management error under aggressive ($H_{max}=0.8$) and more sustainable maximum harvest

rates ($H_{\max}=0.4$). The insensitivity was caused by the fundamental flaw of using aggregate abundance to determine harvest rate. An abundance-based rule based on the aggregate recruitment will still overexploit weak populations regardless of the error in recruitment forecasts. Overexploitation leads to reduced performance in terms of both conservation and yield. Increasing the extent of forecast error has little impact on the frequency of overexploitation, and hence has little effect on performance statistics. Abundance-based harvest rate rules only make sense if their limit reference points are based on the status of the weak populations that they are designed to protect.

Acknowledgements

Thanks to Blair Holtby, Mike Bradford, Michael Folkes, Jim Irvine, Michael Chamberlain, Kent Simpson, Eric Parkinson, Joseph Tadey, Gary Morishima, and Bob Hayman for providing data or useful commentary on this analysis.

References

- Barrowman, N.J., and R.A. Myers. 2000. Still more spawner-recruitment curves: the hockey stick and its generalizations. *Can. J. Fish. Aquat. Sci.* 57:665-676.
- Barrowman, N.J., Myers, R.A., Hilborn, R., Kehler, D.G., and C.A. Field. 2003. The variability among populations of coho salmon in the maximum reproductive rate and depensation. *Ecological Applications* 13(3):784-793.
- Bradford, M.J., Myers, R.A., and J.R. Irvine. 2000. Reference points for coho salmon (*Oncorhynchus kisutch*) harvest rates and escapement goals based on freshwater production. *Can. J. Fish. Aquat. Sci.* 57: 677-686.
- Bradford, M.J. 1999. Spatial and temporal trends in coho salmon smolt abundance in western North America. *Trans. Am. Fish. Soc.* 128: 840-846.
- Bradford, M.J., Taylor, G.C., and Allan, J.A. 1997. Empirical review of coho salmon smolt abundance and the prediction of smolt production at the regional level. *Trans. Am. Fish. Soc.* 126: 49-64.
- Bradford, M.J.. 1995. Comparative review of Pacific salmon survival rates.. *Can. J. Fish. Aquat. Sci.* 52: 1327-1338.
- Chen, D.G., and L.B. Holtby. 2002. A regional meta-model for stock-recruitment analysis using an empirical Bayesian approach. *Can. J. Fish. Aquat. Sci.* 59: 1503-1514.
- Irvine, J.R. Parken, C.K., Chen, D.G., Candy, J. Ming, T., Supernault, J., Shaw, W. and R.E. Bailey. 2001. 2001 Stock status assessment of coho salmon from the interior Fraser River. Canadian Science Advisory Secretariat Research Document 2001/083.
- PSC (Pacific Salmon Commission). 2004. Pacific Salmon Treaty, March 2004. 116 pp.
- Simpson, K. Chamberlain, M., Fagan, J., Tanasichuk, R.W., and D. Dobson. 2004. Forecast for southern and central British Columbia coho salmon in 2004. PSARC working paper.
- Stocker, M. and D. Peacock. 1988. Report of the PSARC Salmon Subcommittee meeting April 27-May 1, 1998. and the Steering Committee meeting May 4, 1998. Canadian Stock Assessment Proceedings Series 98/08. Fisheries and Oceans Canada, Ottawa, Onto.

Walters, C.J., and A.M. Parma. 1996. Fixed exploitation rate strategies for coping with effects of climate change. *Can. J. Fish. Aquat. Sci.* 53:148-158.

Hilborn, R. and C.J. Walters. 1992. *Quantitative fisheries stock assessment*. Chapman and Hall, New York, NY.

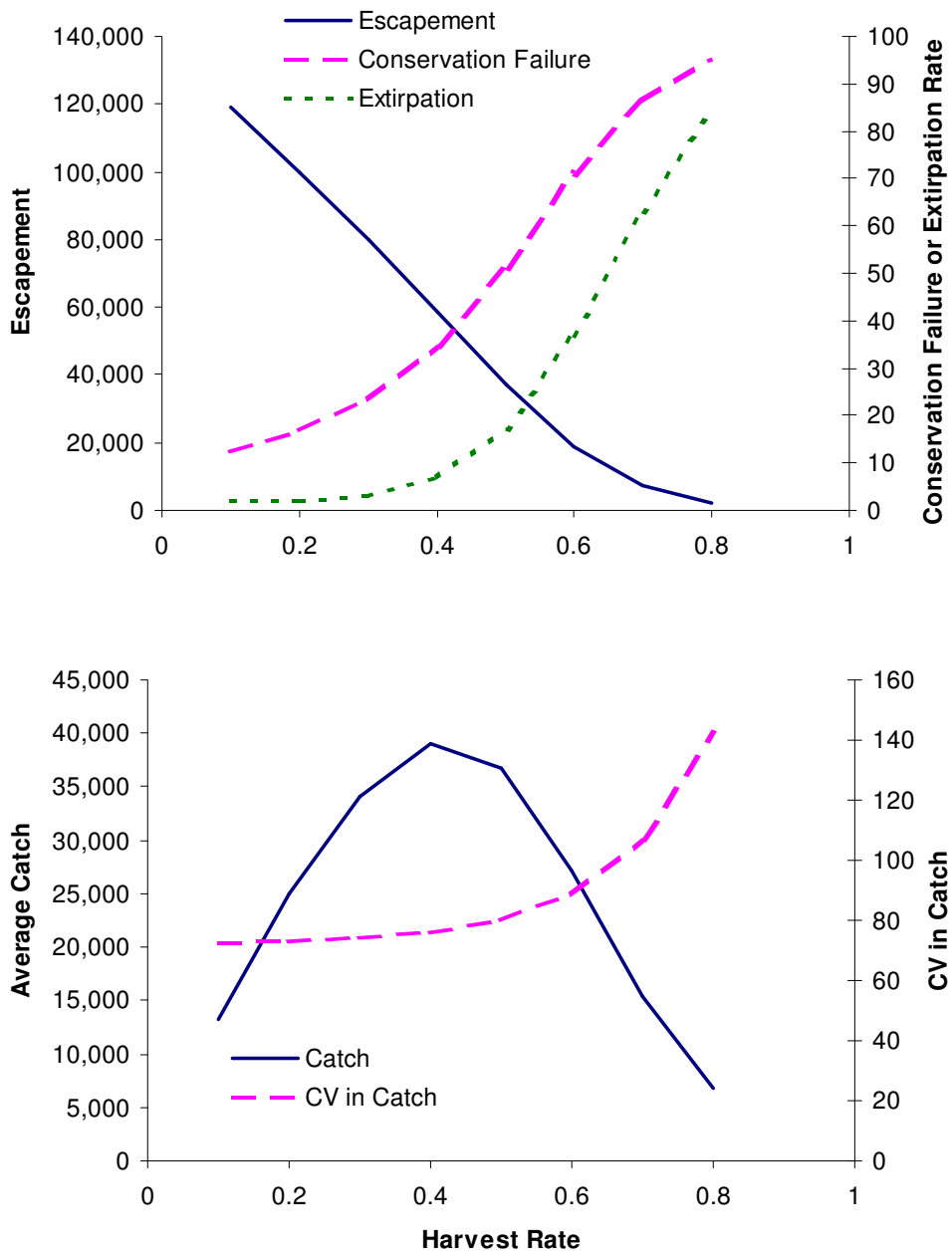


Figure 1. Performance statistics at fixed harvest rates of 0.1-0.8 under default model parameters (Table 1).

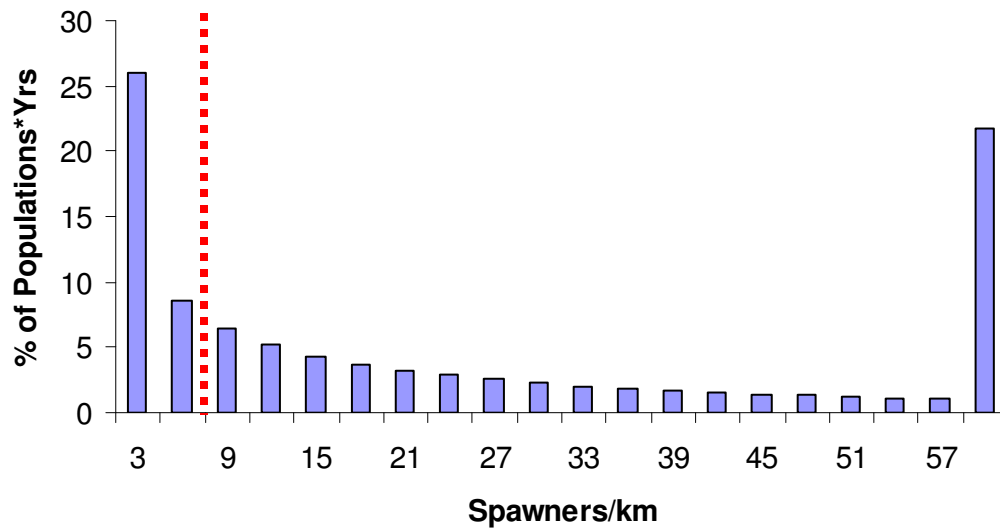
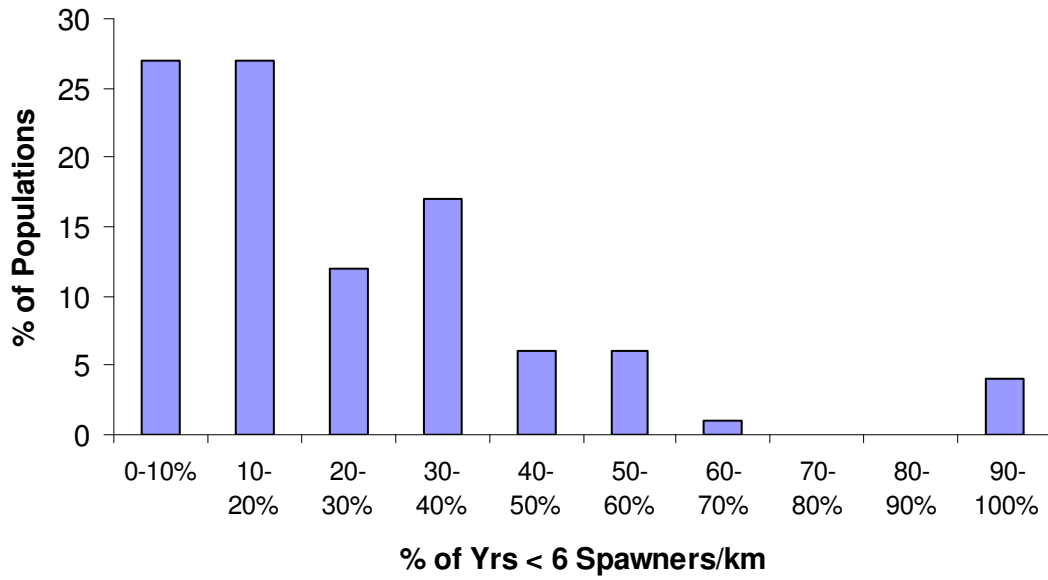


Figure 2. Statistics of the status of 100 populations based on a fixed harvest rate of 0.4 and default model parameters (Table 1). The top graph shows the percentage of populations by conservation failure rate category. The bottom graph shows the distribution of spawner densities across all simulated years and populations with the conservation limit of 6 spawners/km shown for reference (red dashed line). The last bar in the bottom graph represent the % of populations with more than 60 spawners/km. The sum of values below the limit is the conservation failure rate (35% in this example).

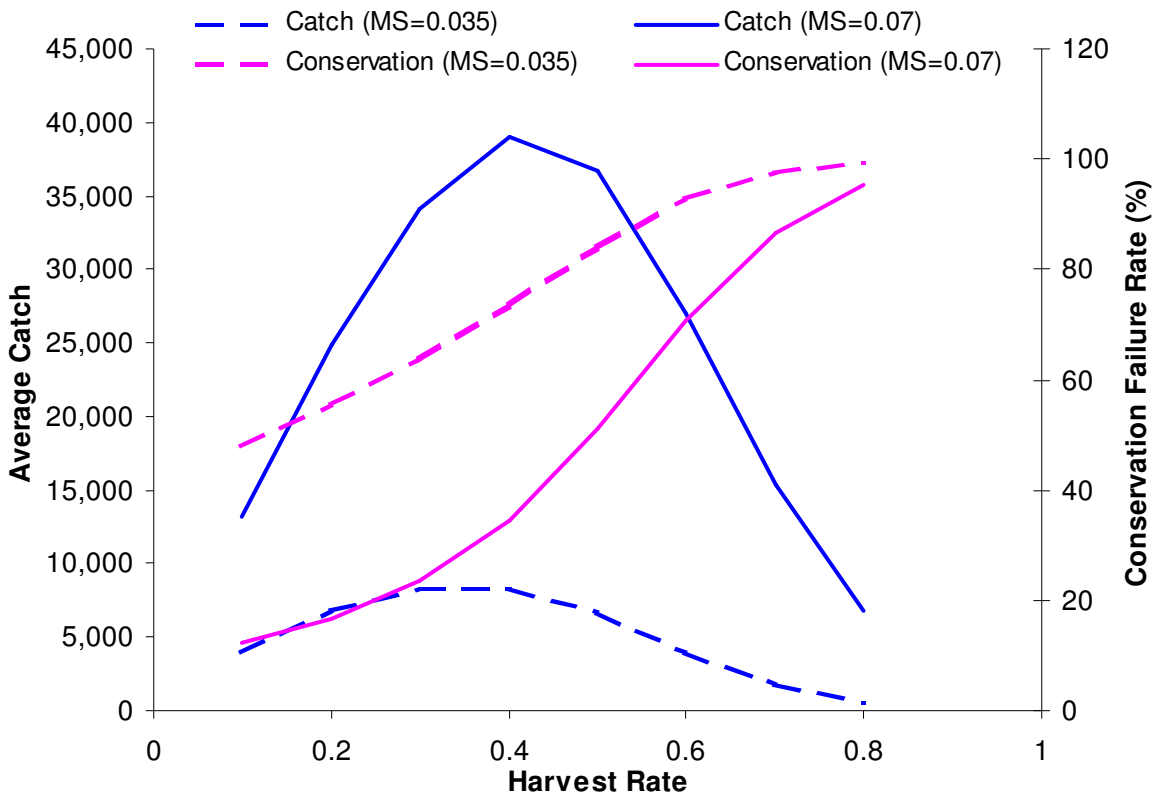


Figure 3. Average catch and conservation failure rate across a range of fixed exploitation rates at low (0.035) and average (0.07) marine survival rates.

Table 1. Summary of default model parameters. SD, FW, and MAR denote standard deviation, freshwater and marine, respectively. Values in parentheses represent non-default values that were evaluated in sensitivity analyses.

Parameter	Symbol	Value	Source
Spawner-to-smolt	α, β	stochastic	From Hierarchical Bayesian Model (HBM) Analysis of Logistic Hockey Stick model
Mean marine survival rate	MS	0.07 (0.035)	Average from 8 index stocks, 1972-2001
SD of FW survival	σ_f	0.33	Median from 17 populations from HBM analysis
SD of MAR survival	σ_m	0.90	Mean of 8 index stocks,
Lag-1 autocorrelation – FW	$\rho_{y,f}$	0.3	Mean lag-1 correlation for 17 populations used in HBM
Lag-1 autocorrelation – MAR	$\rho_{y,m}$	0.65	Mean lag-1 correlation of 8 index stocks
Inter-population correlation – FW	$\rho_{p,f}$	0.39	Correlation among 17 populations used in HBM
Inter-population correlation – MAR	$\rho_{p,m}$	0.65	Correlation among 8 index stocks
SD of recruitment forecast	σ_κ	0.5 (0, 0.75)	Simpson et al. 2004
SD of mean harvest rate	σ_λ	0.25 (0, 0.5)	Uncertain, range of values examined
SD of population specific harvest rate	σ_η	0.25 (0, 0.5)	Uncertain, range of values examined
Conservation failure limit (spawners/km)		6	Stocker and Peacock 1998

Table 2. Performance statistics under fixed- ($Esc_{min}=Esc_{max}=0$) and abundance-based harvest rate policies. Esc, Cons. Fail, Extirpate, Catch, CV Catch, and Avg H refer to the average aggregate escapement, conservation failure rate (%), percentage of populations that are extirpated, average catch, coefficient of variation in catch, and average realized harvest rate, respectively. Results are based on default model parameters (see Table 1). Within each set, the harvest parameters that produced the highest average catch are shown in bold.

Esc_{min}	Esc_{max}	H_{min}	H_{max}	<i>Esc</i>	Cons. Fail	Extirpate	Catch	CV Catch	Avg H
0	0	0.1	0.1	119,144	12	2	13,218	72	10
0	0	0.2	0.2	99,817	17	2	24,911	73	20
0	0	0.3	0.3	79,860	24	3	34,156	74	30
0	0	0.4	0.4	58,768	35	7	39,029	76	40
0	0	0.5	0.5	37,193	51	17	36,725	80	50
0	0	0.6	0.6	18,859	71	37	27,092	89	59
0	0	0.7	0.7	7,488	87	63	15,416	107	67
0	0	0.8	0.8	2,338	95	84	6,836	142	75
7,200	33,600	0.1	0.8	14,061	75	40	23,978	106	63
7,200	67,200	0.1	0.8	22,540	64	27	31,159	109	58
7,200	100,800	0.1	0.8	30,055	56	19	35,602	113	54
25,000	33,600	0.1	0.8	18,458	71	33	25,900	120	58
25,000	67,200	0.1	0.8	26,832	60	23	32,313	121	55
25,000	100,800	0.1	0.8	34,242	52	16	36,224	123	51
7,200	33,600	0.1	0.4	62,163	31	5	39,875	78	39
7,200	67,200	0.1	0.4	67,948	27	4	40,070	84	37
7,200	100,800	0.1	0.4	73,405	24	3	39,327	90	35
25,000	33,600	0.1	0.4	64,345	30	5	40,013	82	38
25,000	67,200	0.1	0.4	70,314	26	3	39,894	88	36
25,000	100,800	0.1	0.4	75,772	23	3	38,906	94	34
7,200	33,600	0.1	0.6	28,492	58	22	34,937	89	55
7,200	67,200	0.1	0.6	38,014	48	14	39,505	95	51
7,200	100,800	0.1	0.6	46,177	41	9	41,658	101	47
25,000	33,600	0.1	0.6	32,455	54	18	36,257	96	53
25,000	67,200	0.1	0.6	41,805	45	11	40,098	102	49
25,000	100,800	0.1	0.6	49,806	38	7	41,740	107	46

Table 3. Performance statistics under fixed- ($Esc_{min}=Esc_{max}=0$) and abundance-based harvest rate policies based on increased and reduced error in recruitment forecasts (σ_{κ}), and implementation of the average (σ_{λ}) and population-specific (σ_{η}) harvest rates. See caption for Table 2 for details.

Esc_{min}	Esc_{max}	H_{min}	H_{max}	σ_{κ}	σ_{λ}	σ_{η}	Esc	Cons. Fail	Extirpate	Catch	CV Catch	Avg H
0	0	0.4	0.4	0.75	0.25	0.25	58,768	35	7	39,029	76	40
7,200	33,600	0.1	0.4	0.75	0.25	0.25	64,752	30	5	39,753	81	38
7,200	67,200	0.1	0.4	0.75	0.25	0.25	71,535	25	3	39,068	88	35
7,200	100,800	0.1	0.4	0.75	0.25	0.25	77,092	23	3	37,720	94	33
25,000	33,600	0.1	0.4	0.75	0.25	0.25	67,882	28	4	39,426	87	37
25,000	67,200	0.1	0.4	0.75	0.25	0.25	74,564	24	3	38,385	94	34
25,000	100,800	0.1	0.4	0.75	0.25	0.25	79,908	21	3	36,860	100	32
0	0	0.4	0.4	0.5	0.5	0.5	48,734	49	13	29,739	93	38
7,200	33,600	0.1	0.4	0.5	0.5	0.5	54,309	43	9	31,542	95	37
7,200	67,200	0.1	0.4	0.5	0.5	0.5	61,647	37	6	32,727	101	35
7,200	100,800	0.1	0.4	0.5	0.5	0.5	68,042	32	4	32,930	106	33
25,000	33,600	0.1	0.4	0.5	0.5	0.5	57,394	41	7	32,016	99	36
25,000	67,200	0.1	0.4	0.5	0.5	0.5	64,658	35	5	32,840	105	34
25,000	100,800	0.1	0.4	0.5	0.5	0.5	70,929	30	4	32,790	110	32
0	0	0.4	0.4	0.5	0	0	62,067	31	6	41,378	69	40
7,200	33,600	0.1	0.4	0.5	0	0	64,854	28	5	41,920	71	39
7,200	67,200	0.1	0.4	0.5	0	0	69,975	25	4	41,712	77	37
7,200	100,800	0.1	0.4	0.5	0	0	74,976	22	3	40,628	84	35
25,000	33,600	0.1	0.4	0.5	0	0	66,850	27	4	41,993	74	39
25,000	67,200	0.1	0.4	0.5	0	0	72,205	23	3	41,477	81	36
25,000	100,800	0.1	0.4	0.5	0	0	77,239	21	3	40,153	88	34

Table 3. Con't

Esc_{min}	Esc_{max}	H_{min}	H_{max}	σ_K	σ_λ	σ_η	<i>Esc</i>	Cons. Fail	Extirpate	Catch	CV Catch	Avg H
0	0	0.4	0.4	0.5	0.25	0	60,984	32	6	40,547	75	40
7,200	33,600	0.1	0.4	0.5	0.25	0	63,994	29	5	41,202	78	39
7,200	67,200	0.1	0.4	0.5	0.25	0	69,336	25	4	41,133	84	37
7,200	100,800	0.1	0.4	0.5	0.25	0	74,486	23	3	40,162	90	35
25,000	33,600	0.1	0.4	0.5	0.25	0	66,062	28	4	41,304	81	38
25,000	67,200	0.1	0.4	0.5	0.25	0	71,614	24	3	40,925	87	36
25,000	100,800	0.1	0.4	0.5	0.25	0	76,787	21	3	39,710	94	34
0	0	0.4	0.4	0.5	0	0.25	60,820	32	6	40,552	69	40
7,200	33,600	0.1	0.4	0.5	0	0.25	63,817	29	5	41,198	72	39
7,200	67,200	0.1	0.4	0.5	0	0.25	69,188	25	4	41,138	78	37
7,200	100,800	0.1	0.4	0.5	0	0.25	74,367	23	3	40,179	84	35
25,000	33,600	0.1	0.4	0.5	0	0.25	65,883	28	4	41,296	75	39
25,000	67,200	0.1	0.4	0.5	0	0.25	71,474	24	3	40,928	82	36
25,000	100,800	0.1	0.4	0.5	0	0.25	76,674	21	3	39,726	88	34